

Optics and Photonics Research for Montana Economic Development - MREDI Project Quarter 7 – May 6, 2017

Principal Investigator: Joseph A. Shaw (joseph.shaw@montana.edu)

Coinvestigators: Ross Snider (rosss@montana.edu), Rick Lawrence (rickl@montana.edu), Neda Nategh (neda.nategh@montana.edu), Zeb Barber (barber@montana.edu), Ed Dratz (dratz@montana.edu), Chris Arrasmith (arrasmith@revibrooptics.com), Rufus Cone (rufus.cone@montana.edu), Kevin Repasky (repasky@montana.edu), Rob Walker (rawalker@montana.edu).

Introduction

This project is on schedule and within budget, and is continuing to enable important collaboration between the optics and photonics research and business communities.

Subproject 1: Ultra-compact spectral imagers for precision agriculture and mapping of wildfires and natural resources (Joseph Shaw, joseph.shaw@montana.edu, with NWB Sensors, Inc.). Development of ultra-compact imaging systems for weed mapping in precision agriculture, UAV mapping of wildfires, and a wide variety of ground-based and airborne remote sensing.

Milestones

- a) September 30, 2015: Initial agricultural data collection completed
- b) December 31, 2015: Initial weed maps complete
- c) June 30, 2016: Prepare a refined imaging system and application-specific algorithm
- d) December 31, 2016: Complete results of summer 2016 harvest experiment
- e) June 30, 2017: Finish imaging system and algorithms and transfer to private partner

Introduction

During the seventh-quarter of this subproject we focused on beginning to wrap up the research activities by documenting progress and procedures, publishing results, arranging licenses to commercial partners, and studying the market for commercial products resulting from this research.

Weed mapping

Documentation

For the weed-mapping subproject, we created manuscripts providing full documentation of our software and data sets to be transferred to our commercial partner, NWB Sensors, Inc. We identified problem areas within the current weed mapping process that need improvement and investigated methods of data processing to improve our algorithms. Manuscripts have been created for each script and algorithm used throughout this project, which will assist future research. The original and experimental data sets have been thoroughly documented. These documents include file locations, experiment processes, and results.

New areas of research and experimentation could increase the performance of the weed mapping process. Some of these areas include algorithm improvement, new data processing techniques, and larger training sets. Existing algorithms were not able to process all of the data collected in 2015 and 2016. There were a few data sets collected on hilly terrain that caused the cameras to capture images of the sky, for example. The existing algorithms cannot process these images due to the changing region of interest. Implementing larger training sets could improve the detection capabilities of the current machine learning algorithms.

Normalized Difference Vegetation Index (NDVI) Imagery

During our initial tests of the Raspberry Pi RGB and NDVI data collected during the 2016 harvest, we found that much of the image data appeared too dark. Our concern was that these dark images had a low dynamic range and would not contain any valuable sensor information. However, after further investigation, we found that images could be processed to increase their dynamic range. Therefore, we intentionally processed dark images collected during dusk and were successful at extracting RGB and NDVI sensor information. Lighting issues in the weed detection process have proven to be challenging in this research, and solving lighting issues in imagery will improve results in the future.

The raw Raspberry Pi camera images shown in Figures 1.1 & 1.2 illustrate the steps we used to process images to increase their dynamic range. These initial attempts were successful and we found that we could increase image brightness without injecting noise into the image data. Reprocessing these images with a higher dynamic range means we have the ability to detect weeds in a larger set of images.



Figure 1.1. Modified Raspberry Pi v1.3 RGB image containing weeds.

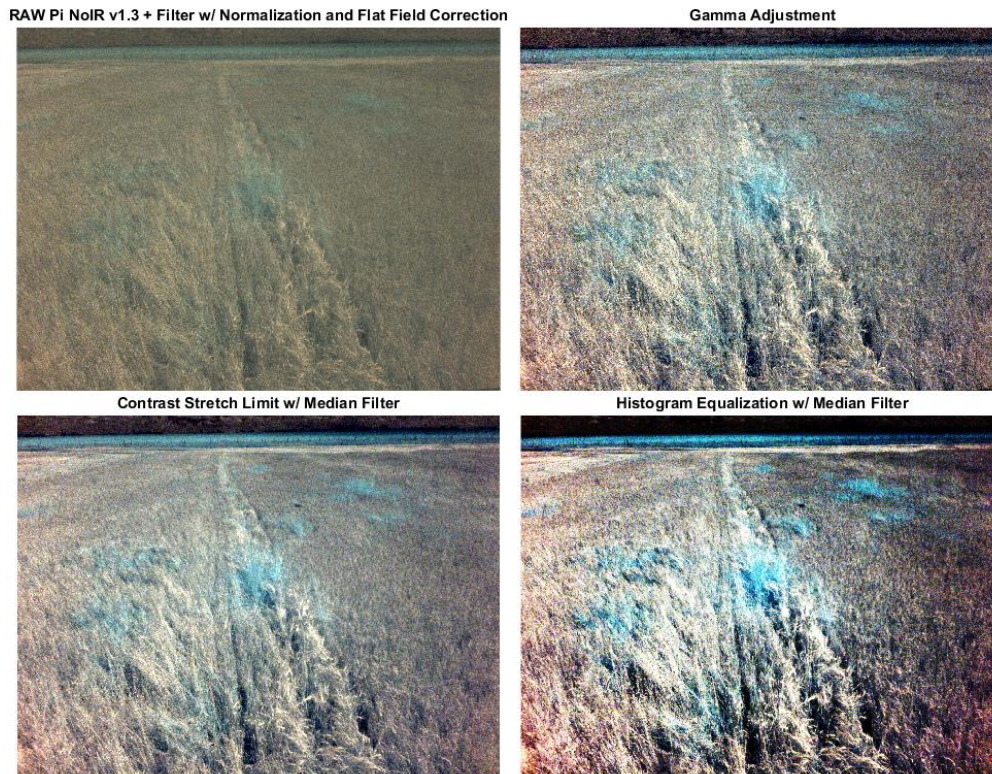


Figure 1.2. Modified Raspberry Pi v1.3 NoIR + custom filter image containing weeds.

We also applied updated methods using an automated data acquisition system for measuring the relative spectral response curves for the Raspberry Pi v2.1 cameras. Results are shown in Figures 1.3, 1.4, and 1.5. This automated system also has the ability to collect spectral response data on different cameras in the future. These measurements suggest that research being performed by several groups around the world may have some inaccuracies that will be reduced by our measurements. Therefore, these results are being prepared for publication.

The spectral response in Figure 1.3 was collected on the Pi v2.1 camera, which is very similar to the Pi v1.3 camera that captured the image in Figure 1.1. The spectral graph in Figure 5 shows the blue filter cutting off spectral response of the NoIR camera below 600 nm. This spectral response is similar to the Pi v1.3 cameras used to collect the image data shown in Figure 1.2.

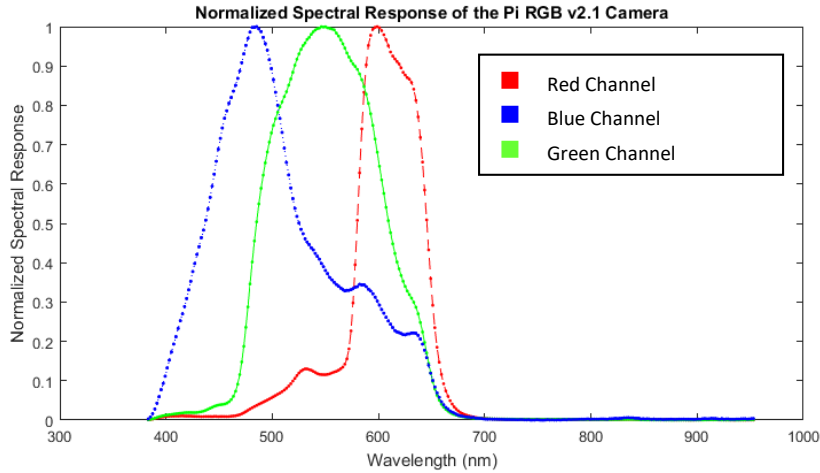


Figure 1.3. Relative spectral response of the Raspberry Pi v2.1 RGB Camera (with infrared-blocking filter).

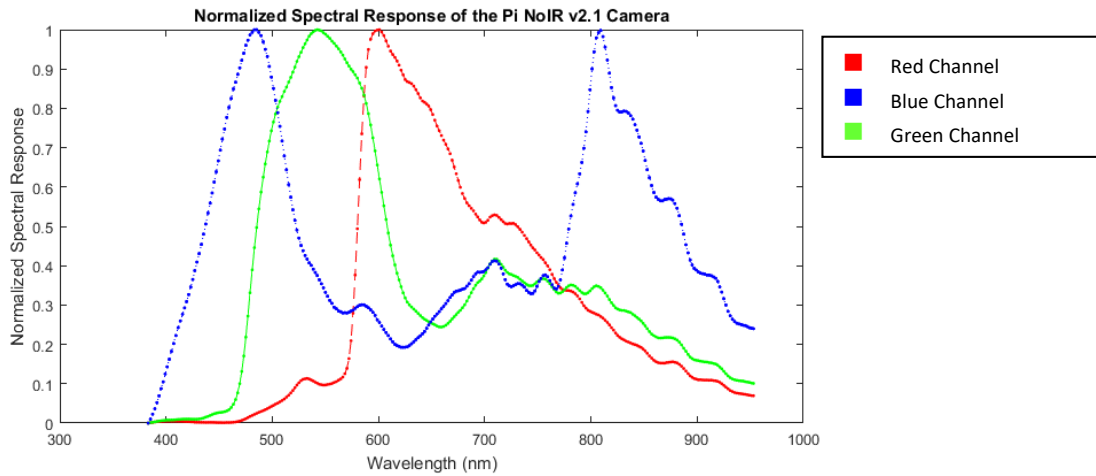


Figure 1.4. Relative spectral response of the Raspberry Pi v2.1 NoIR Camera (no infrared filter).

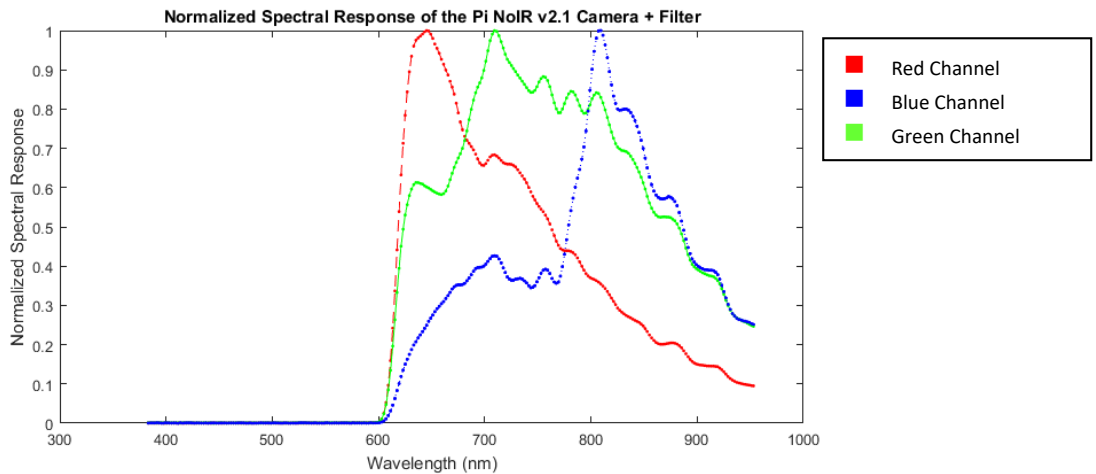


Figure 1.5. Relative spectral response of the Raspberry Pi v2.1 NoIR Camera with blue-blocking filter but no infrared-blocking filter.

Wireless Ultra-Compact IR Imager

We created a mobile version of the FLIR Lepton thermal camera system by modifying the Raspberry Pi it was previously operating from to act as an access point. Any Wifi-capable computer or cellphone can now connect to the Raspberry Pi and view the Lepton sensor data in real-time. We were able to integrate a push button into the system to capture images and store them to a USB drive. A photograph of the system is shown in Figure 1.6a and a sample thermal IR image is in Figure 1.6b.

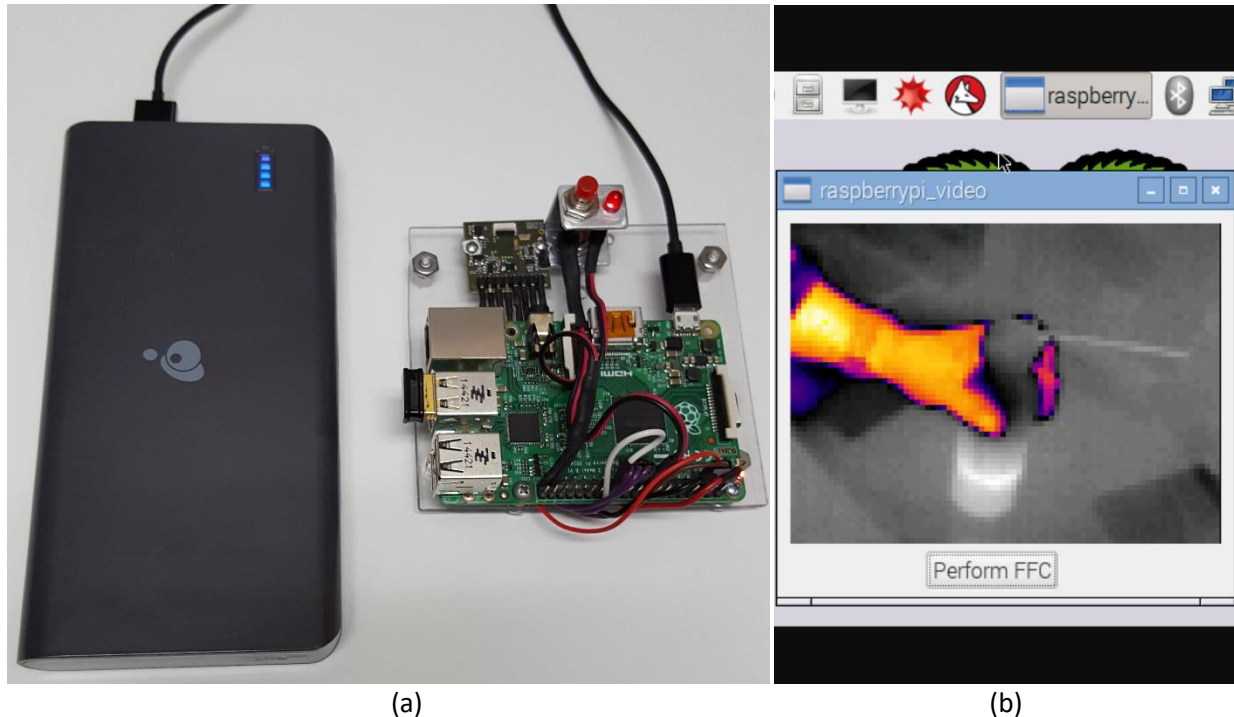


Figure 1.6. (a) Raspberry Pi with FLIR Lepton powered by battery pack; (b) Lepton broadcasting image data via Wifi to cellphone.

Ultra-compact weed imager market study

This subproject is tasked with performing a commercialization and market study for the technology developed under the MREDI Subproject 1 titled “Ultra-compact spectral imagers for precision agriculture and mapping of wildfires and natural resources.” This portion of the project, focusing on optical weed mapping technology, is being done on a subcontract to NWB Sensors, Inc. (NWB) as the commercialization research partner. Although funding details had not yet been completed as of October 2017, NWB had expressed interest to pursue this technology and with the oversight of MSU Research Compliance and MSU Technology Transfer, NWB submitted an SBIR Phase I proposal to USDA/NIFA. NWB has been informed that our proposal has been recommended for funding, and NWB is finalizing the details of a license for the weed mapping technology and data from the MREDI Optics project.

Market research

With the commercial license moving forward, NWB is continuing the market research work specified in the MREDI Optics program. An initial assessment of the market shows many companies trying to bring

precision mapping systems to agriculture. Despite this, initial discussions with Montana farmers shows that these technologies are not being utilized. Feedback from experts in the field have suggested that precision agriculture has eluded the small and mid-size farms because of economies of scale and cost-benefit balance. To successfully bring this technology to market, we are working to understand these aspects of precision agriculture and determine if the MSU-developed technology can avoid these hurdles, and find its way into the hands of Montana farmers.

Part of this study has been to develop an understanding of the performance of the MSU mapping technology to better understand its competitive advantages in the market. To this end, NWB has hired a new employee with a strong background in computer science and machine vision, gained in part through his graduate work in the MSU Computer Science Department. Strengths we have identified for the MSU technology are:

- 1) The low cost of the cameras for mapping. This low cost allows lower value-per-acre crops (such as wheat) to be targeted.
- 2) The low level of added work to the farmer. The cameras have been mounted inside the farmers' equipment with no modifications required for the equipment.
- 3) MSU's mapping technology started with real-world data collected from combines during harvest, so the technology was developed based on data that contained lighting variations, dust, and unknown non-target objects in the field; therefore, the performance of these algorithms in the real-world is already known.

These strengths may give this technology a competitive advantage over existing technologies.

Professional consultant

This project included funding for a professional commercialization consultant. NWB Sensors, Inc. is using the Montana Manufacturing Extension Center (MMEC) as this consultant and will go through their Technology-Driven Market Intelligence (TMDI) program. Initial discussions began with MMEC in March 2017 to understand the technology developed under MREDD support and to understand the markets in which NWB Sensors, Inc. sees a fit for this technology.

Airborne Lidar

A design study for the airborne lidar that was partly developed, refined, and deployed with support from this project was published this quarter. One other paper has been submitted for publication, and a third will be submitted during the next quarter. Michael Roddewig successfully defended his Ph.D. dissertation, "Airborne lidar applications in freshwater lakes," in April 2017.

Expenditures to date (Grant 41W410) Personnel \$156,160.63, Benefits \$41,598.94, Operations \$48,826.21, Sub Award \$205,208.79; total Expenditures **\$451,794.57**.

Subproject 2: High-performance, real-time image processing for hyperspectral imaging (Ross Snider with Resonon, Inc.) Design a high-speed hyperspectral waterfall sorting system to fuse object edge information with hyperspectral data to sort agricultural products quickly and efficiently using Resonon's Hyperspectral Imagers and remove rejected items via air jets. The goal is to perform the data fusion, accept/reject decision, and removal, all in real-time using FPGA technology.

Milestones

- a) February 1, 2016: Determination of center of mass of each food item in image/line scan
- b) September 1, 2016: Determine trajectory of food item for precise timing removal
- c) February 1, 2017: Integrate hyperspectral data within food item edge boundaries
- d) June 31, 2017: Use hyperspectral data within food item edges to classify food item as accept/reject
- e) June 31, 2017: Time air jets to remove rejected food items
- f) June 31, 2017: Final report emphasizing commercial products and potential

Activities to date

Objective 4: Design a high-speed hyperspectral waterfall sorting system to fuse object edge information with hyperspectral data to sort agricultural products quickly and efficiently using Resonon's hyperspectral Imagers and remove rejected items via air jets.

- 1. Connor Dack successfully defended his Master's Thesis. As a result of his FPGA work, Connor was just hired by the local Bozeman company Flat Earth, Inc. The FPGA smart camera development work is likely to be licensed to Flat Earth, who will make this smart camera for Resonon, Inc. Figure 2.1 is a copy of the announcement of his thesis defense.

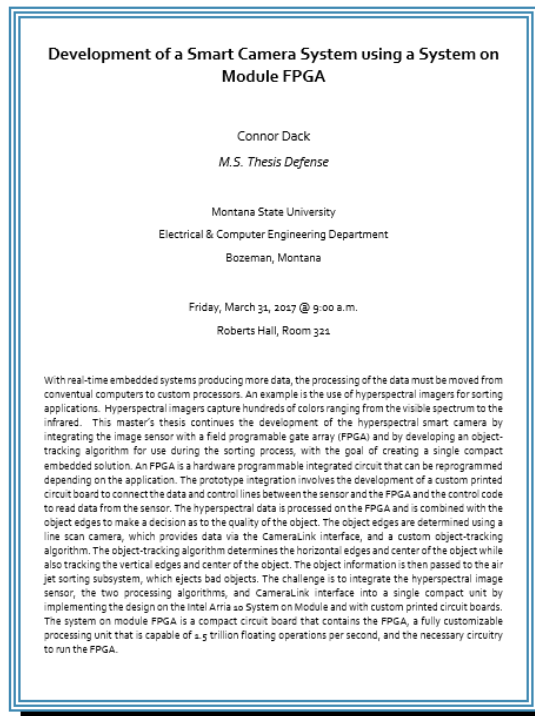


Figure 2.1. Announcement of Connor Dack's MS thesis defense on 31 March 2017.

2. The air jet system has been successfully completed by the senior design group comprised of Sam Kysar, Molly Tomlinson, and Phillip Lowther. This system was demonstrated at the College of Engineering Senior Design Fair on Thursday, April 27, 2017. Figure 2.2 is a copy of their poster.



Hyperspectral Waterfall Sorting

Phillip Lowther, Sam Kysar, Molly Tomlinson
Faculty Advisor: Dr. Ross Snider

Sponsors: Montana Research and Economic Development Initiative (MREDI),
Montana Board of Research and Commercialization Technology (MBRCT), Resonon, Dr. Ross Snider




Introduction

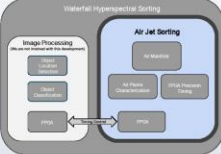
This project began two years ago in 2014 with a sponsorship from Resonon and MBRCT. The project consisted of a hyper-spectral camera and a PC to process images of almonds and have a robotic arm physically remove almonds characterized as "bad". During the year of 2014 a senior design team of four moved the processing to Field Programmable Gate Arrays (FPGA). A team of two from the senior design class of 2015-2016 created an object detection algorithm which would detect a falling object (Almond) and find it's center of mass while it was in free-fall.



In 2016, the Montana Research and Economic Development Initiative sponsorship led to the possibility of bringing this project to market as a feasible alternative for local farmers to sort their own crops. The goal for this project is to sort falling objects in real time.

Objectives

Hyperspectral Waterfall Sorting



- 32 Air Jet Manifold
 - Controlled and timed correctly by I/O of an FPGA
- Precision Timing
 - FPGA to control timing of air jets
- Air Plume Characteristic
 - Latency
 - Visualize plume
- Mount Everything
 - Manifold, and vibratory feeder
- Test and Verification
 - Verifying that everything is working correctly



Air Jet Manifold

As a requirement from the objectives section, a manifold needed to be built and designed such that the air jets span across the four inch drop tray of the vibratory feeder shown in the image in the objectives section. This was to include 32 air jets which were to be fired independently at precise timing and as needed. From early designs (below, left) a new design was created designed and then built (below, right).





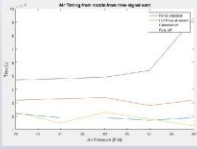
Early Design Final Design Exploded View

The final manifold build included 32 holes at 1/16" diameter spaced by an 1/8" each of which can be fired independently.

Air Plume Characterization using Schlieren Optics

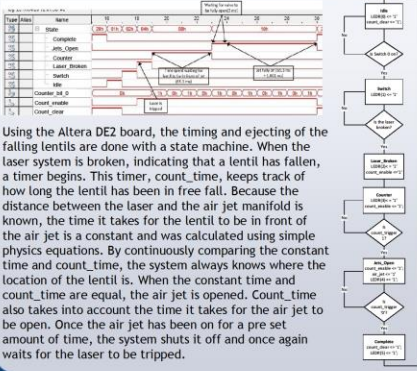
In order to characterize the air plume, two systems were needed. This characterization was completed by designing, building, and testing a Schlieren optics setup (below) and a force sensor (right) to detect latency.

The force sensor was used to detect a voltage change and plot this voltage reading against time to accurately determine the timing (on/off) which is shown in the picture to the right. Using a voltage divider circuit and an analog to digital converter, the latency from an air jet was accurately plotted against time, and is shown in the FPGA Precision Timing box.

The Schlieren optics setup was used to visualize the air plume from the manifold interacting with a lens. This was desired because the team needed to know exactly how long to leave the air jet on for. It also allowed the team to view exactly how the lentil would react at certain pressures and durations.

FPGA Precision Timing



Using the Altera DE2 board, the timing and ejecting of the falling lentils are done with a state machine. When the laser system is broken, indicating that a lentil has fallen, a timer begins. This timer, count_time, keeps track of how long the lentil has been in free-fall. Because the distance between the laser and the air jet manifold is known, the time it takes for the lentil to be in front of the air jet is a constant and was calculated using simple physics equations. By continuously comparing the constant time and count_time, the system always knows where the location of the lentil is. When the constant time and count_time are equal, the air jet is opened. Count_time also takes into account the time it takes for the air jet to be open. Once the air jet has been on for a pre set amount of time, the system shuts it off and once again waits for the laser to be tripped.



Figure 2.2. (top) Poster presented at the MSU Engineering Design Fair on 27 April 2017; (bottom left) photo of senior design team of Sam Kysar, Phillip Lowther, and Molly Tomlinson; (bottom right) sorting system that can open and shut an air valve in milliseconds to hit a falling lentil.

- The mSATA FPGA Controller has been successfully completed by the senior design group comprised of Nick Lapp, Hendrick Haataja, and Hannah Mohr. This system was demonstrated at the College of Engineering Senior Design Fair on Thursday, April 27, 2017. The poster for this project is shown in Figure 2.3.



6.0 Gbps mSATA FPGA Controller

Hendrick E. Haataja, Nickolas W. Lapp, Hannah D. Mohr
Electrical and Computer Engineering, Montana State University, Bozeman, MT, USA

Abstract

A 6.0 gigabit per second (Gbps) Serial Advanced Technology Attachment (SATA) interface is presented. This memory interface is designed and implemented for the Altera Cyclone V ST Field Programmable Gate Array (FPGA) and is compliant with SATA 3.1 protocol specifications. Design features include a simple, abstracted application interface, 200 megabytes per second (MBps) sequential write speeds, robust data transmission and error handling, and lightweight, low cost hardware suitable for airborne applications. Final implementation enables an abstracted, reusable link between FPGA applications and nonvolatile memory and will be used to save hyperspectral images from an airborne imaging system in development by Resonon technologies.

Results

Performance Metrics

Link Speed: 6.0 Gbps
Write Speed: 200 MBps
Read Speed: 150 MBps
Error Rate: 1.8×10^{-7} errors/dword

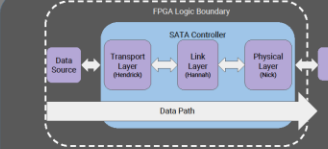
Performance characterized by writing 2048 dword blocks of sequential counter data

Resource Utilization

Logic Utilization: 5% (2061 ALMs)
Block Memory Bits: 3% (148 kb)
XCVR Pairs: 11% (1/9)
Total PLLs: 13% (2/15)
Clock Speed: 150 MHz
Lines of Code: 7,072

Resource Percentages based on Cyclone V STFD6

Method



Design broken into four layers: Application, Link, Transport, Physical

- Application Layer: Receive data and control signals from user
- Transport: Transform data into a Frame Information Structure (FIS)
- Link: Scramble/Encode Data
- Physical: Convert low-speed parallel to high-speed serial data

Background

- SATA is the protocol that governs reads and writes between hosts (computers) and clients (SSDs and Hard Drives)
- This project involved the design and implementation of a SATA host controller on a Cyclone V ST FPGA
- Design is low-cost, flight-capable, high-throughput memory controller



This project enables many FPGA designs, including:

- Airborne Hyperspectral Imaging System (pictured above)
- Recording of Lentic Images for Camera Characterization
- High-Speed Data Storage and Inspection Module

Verification



Sierra m6-1 Protocol Analyzer:

- Confirm sent frames conform to SATA protocol
- Detect/Debug protocol errors
- Quantify read/write speeds



SignalTap Logic Analyzer was used to debug internal signals, tracing data flow from the application layer to the physical layer.

Conclusions

- Designed and implemented a robust, lightweight, abstracted SATA III Core, the first open-source core developed for the Cyclone V ST FPGA
- Low-cost hardware enables high-speed memory link in budget constrained applications
- Small footprint enables SATA core as addition to complex projects without impinging on resource availability
- Fully met each level 1 requirement, and exceeded write speed requirements by a factor of four

References and Acknowledgments

Support for this project was provided by Dr. Ross Snider, Connor Dack, and the Electrical and Computer Engineering department. Funding for this project was provided by Dr. Ross Snider, Resonon, and the Montana Research and Economic Development Initiative.

Spring 2017

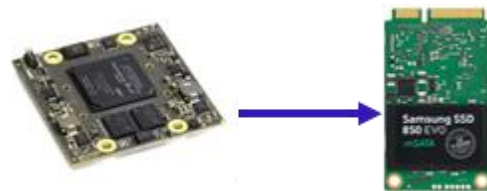
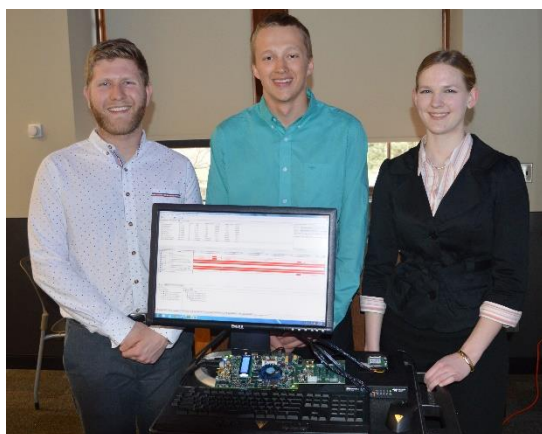


Figure 2.3. (top) Poster presented at the MSU Engineering Design Fair on 27 April 2017; (bottom left) photo of the senior design team of Nick Lapp, Hendrick Haataja, and Hannah Mohr; (bottom right) graphic illustrating that the group successfully demonstrated writing data from a Cyclone V ST FPGA to a SSD at 200 Mb/s.

Activities associated with “hyperspectral imaging for monitoring metabolic state of live cells” (Subproject 6)

Work has been done to control the microscope stage and perform autofocus. Several autofocus algorithms were tried and a local measure of edge sharpness, computed over the entire image, seemed to work the best.

Expenditures to date (41W411)

Personnel to date \$71,597.31, Benefits \$4097.48, Operations \$87,573.68, Capital equipment \$4845.00; Total Expenditures **\$168,113.47**.

Subproject 3: Remote Sensing Algorithms for Precision Agriculture (Rick Lawrence with Resonon, Inc.)
Develop and apply a methodology using hyperspectral imagery for determining optimal narrow spectral band combinations for identifying targeted invasive weeds in specific crops.

Milestones

- a) July 31, 2016: Collect invasive weed field data
- b) August 31, 2016: Collect hyperspectral image data
- c) October 31, 2016: Complete image preprocessing
- d) January 31, 2017: Complete analysis of spectral band optimization and weed species mapping
- e) June 30, 2017: Final report, including applications for commercial site-specific agriculture

Activities to date:

- Generated simulated "broad-band" data at 12, 24, 48, and 96 nm band widths
- Performed band optimization analysis for each bandwidth
- Evaluated weed classification results for optimal bands using multiple machine-learning classification techniques
- Compared results for statistically significant differences
- Evaluated three approaches for atmospheric correction of hyperspectral data

We completed our initial analyses for using select, "optimal" bands to differentiate weeds from a wheat crop. The analyses included four optimization routines, seven machine-learning classification methods, three alternative atmospheric correction techniques, and five different bandwidths, resulting in 420 classifications. Each classification output a map of weed locations (figure 3.1). Best results generally were generated using the narrowest bands, atmospherically corrected to surface reflectance using Landsat satellite imagery, and classified with the random forest algorithm. This combination generally resulted in accuracies of 70-77%. The few exceptions to these combinations did not result in substantially better accuracies. Random forest is able to provide reliable internal accuracy assessments with all data used to train the algorithm. The data initially were split between training the classification algorithms and validating the results so that all algorithms could be compared on the same basis. We repeated the analyses using random forest with all data to determine whether this would improve classification accuracy. Our results indicate a substantial decrease in accuracy from any broadening of the bandwidth (figure 3.2). These initial results indicate that narrow-band sensors have the ability to provide substantially higher abilities to differentiate weeds from crops than broad-band sensors.



Figure 3.1 Weed map resulting from random forest classification using 3 optimal bands selected with Jefferies-Matusita

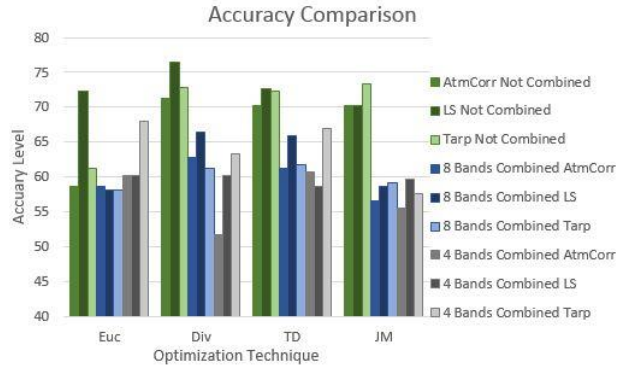


Figure 3.2 Comparison of accuracy between uncombined and groups of 4 and 8 bands.

Expenditures to date (Grant 41W417) Personnel \$44,673.02, Benefits \$2,716.54, Operations \$12,161.44; total Expenditures **\$59,718.00**.

Subproject 4: Machine Vision Algorithms for Precision Agriculture (Neda Nategh) Develop machine vision algorithms for weed detection and food sorting using spectral imaging data.

Milestones

May 31, 2017 Final testing and development complete.

June 30, 2017 Final report completed.

Progress toward objectives

- Students were advised on the analysis of hyperspectral image data and statistical modeling

A new grant proposal is planned to submit based on a similar idea proposed in the MREDI Optics project.

- “Space image processing on images captured by the stereo orbital debris telescope/CCD camera developed by NASA Marshall Space Flight Center” – NASA – Dual Use Technology Development: NASA Marshall Space Flight Center – \$100,000.

Expenditures to date (Grant 41W413) Personnel \$74,009.29, Benefits \$5,651.91, Operations \$10,802.90; total Expenditures **\$90,464.10**.

Subproject 5: Microcavity sensors for hyperspectral imaging (Zeb Barber with Advanced Microcavity Sensors LLC). Advance MSU/Advanced Microcavity Sensors LLC (AMS) technology on microcavity hyperspectral imaging sensors toward commercial applications in agriculture and engineering tests to determine feasibility of mounting sensor technology on UAV; secondary objective solving MT problems in agriculture and biomedical (skin cancer). The primary objective focused on MREDI goal #2: creating private sector jobs.

Milestones

- a) June 1, 2016: Investigate non-circular symmetric micro-cavity mirrors for transverse mode manipulation
- b) September 1, 2016: Evaluate Microcavity Hyperspectral Imaging prototype system for early crop disease/weed detection
- c) December 30, 2016: Determine engineering specifications for use of Hyperspectral Sensor on UAV

Related Funding Summary

No Updates

Personnel Summary

No Updates

Additional Highlights Summary

- The MSU and AMS team met with Richard Harjes of Next Frontier Capital to discuss the commercialization goals of the microcavity technology.

Project introduction

Liquid Crystal Arrayed Microcavities (LCAM) are a new hyperspectral technology invented at Montana State University Spectrum Laboratory (MSU-SL). At the core of this revolutionary technology lie pico-liter volume optical cavities that exploit liquid crystal birefringence for tuning the effective cavity length, producing ultra-fine spectral resolution (~1 nm.) MSU filed for a patent on this technology in 2015 and licensed the technology to Advanced Microcavity Sensors (AMS), which is a Montana licensed company and founded by one of the inventors of the technology. In addition to the MREDI funds, this effort has received funding from: the Montana Board of Research and Commercialization Technology (MBRCT); United States Air Force Small Business Technology Transfer Phase I and Phase II grants awarded to Spectral Molecular imaging, a California company; and a National Science Foundation (NSF) Small Business Innovation Research (SBIR) grant awarded to AMS. MSU-SL received subcontracts from all the previous awards. To date, we have fabricated a variety of LCAM units that performed highly effectively as sub-nm spectral resolution filters in a low-cost, compact, and robust package. Utilizing well-established microfabrication, thin film deposition, and wafer techniques we developed a process for rapidly producing LCAM prototypes.

In June of 2015, Dr. David Atherton joined the LCAM team. He performed a significant amount of the early LCAM development work on the AF STTR and MBRCT work. Dr. Atherton built and tested the first monolithic single channel LCAM units, which contributed to an AF SBIR Phase II being awarded. The goal of the Phase II is to retrofit existing confocal microscopes with a single channel LCAM unit to introduce spectral capabilities. In May for 2016, Dr. Caleb Stoltzfus joined the LCAM team at MSU. He extended

and refined the initial LCAM unit design significantly. Dr. Stoltzfus has also collected and analyzed an enormous amount of data for characterizing LCAMs.

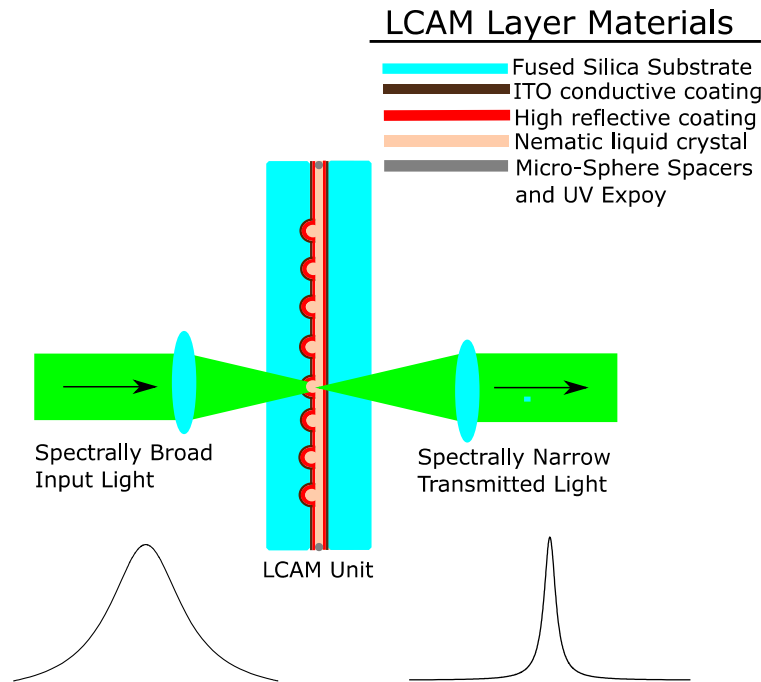


Figure 5.3 Overall concept design for the Liquid Crystal Arrayed Microcavities subproject.

One of the most appealing aspects of the LCAM technology is its architectural elegance. Its deceptive simplicity engenders both functional flexibility with structural ruggedness. The overall concept design for the results presented within this report is depicted in Figure 5.3. Spectrally broad light is coupled to a single LCAM cavity with a microscope objective lens. The transmitted light is irradiated onto a silicon photodetector for measuring cavity properties such as finesse, free spectral range (FSR), the cavity Q factor, and spectral resolution.

The LCAM fabrication process starts with Advanced Microcavity Sensors (AMS) laser ablating arrays of craters onto fused silica wafers, Figure 5.4, which create the substrate for the curved mirrors of the LCAM units. Next, the prepared substrates are sent to Optical Filter Source (OFS) in Austin Texas, who provide the thin film coatings. First, OFS deposits a uniform layer of Indium Tin oxide onto the wafers. Second, OFS applies a highly reflective mirror coating with a mechanical mask that leaves some areas of the ITO coating exposed. After the coatings have been deposited, OFS ships the wafers to MSU Spectrum Lab. The next step in the fabrication process is spin coating a thin film of polymer (PVA or PMMA) onto the flat mirror wafers. The polymer layer serves as an alignment mechanism for the Liquid Crystal (LC) directors. Figure 5.5 (A) contains a photograph of a completed wafer. Spectrum Lab contracts with a neighboring company AdvR to dice the wafers into individual square mirrors, Figure 5.5 (B). Lastly, Spectrum lab assembles the LCAM units and fills them with LC. A gap between the two mirrors is achieved by cementing the mirrors together with UV epoxy that has microsphere spacers of a known diameter mixed in. Figure 5.4 shows a mounted LCAM unit.

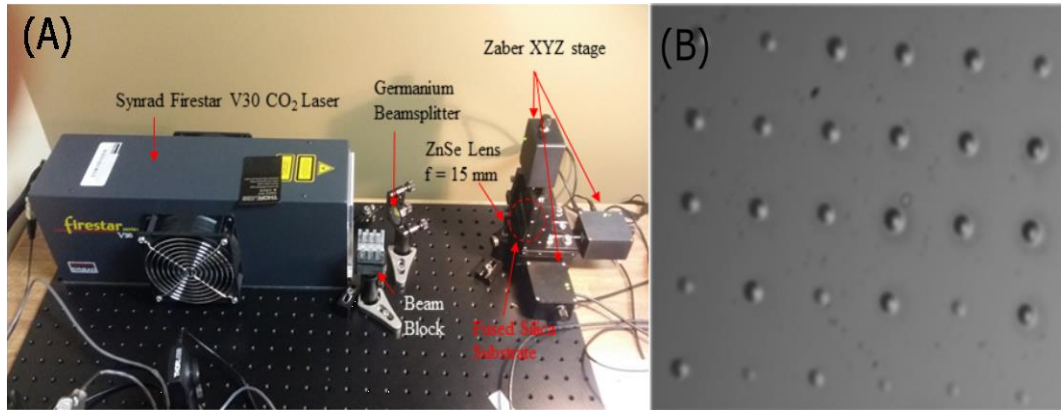


Figure 5.4 (A) AMS's ablation system. (B) An optical microscope image of an array of craters

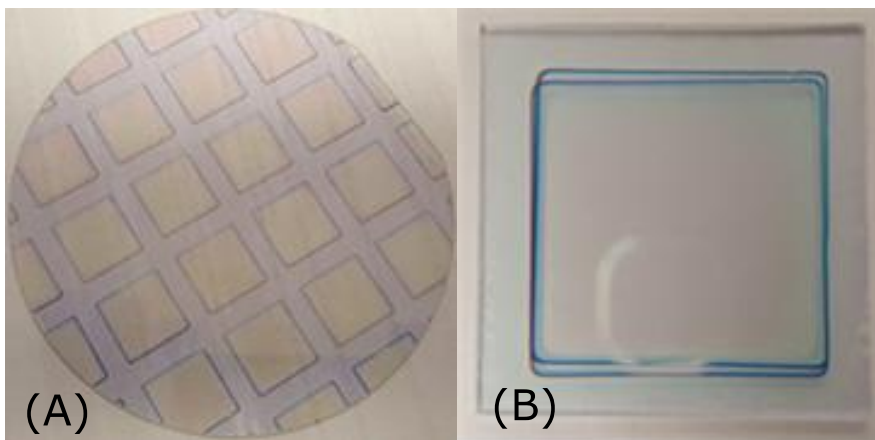


Figure 5.5 (A) Fused silica wafer following deposition of thin film coatings. (B) An individual mirror after the wafer dicing process.

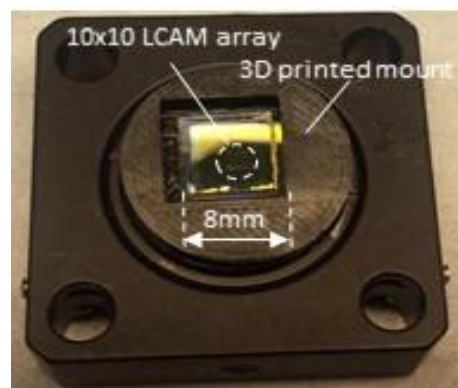


Figure 5.6 An LCAM unit mounted within a custom 3D printed package. The package has an outer diameter of 1", which conveniently fits within generic 1" optics mounts.

Technical progress toward objectives

About 6 months into the project, the goals were changed from the original three objectives. There are now two primary goals for this effort. The first objective is like the original objective a), and is to improve the laser ablation process of creating the arrayed micro-cavities. In particular, we want to

modify the shape of the ablated craters to improve the performance of the device and/or to add different functionality. The second objective replaced b) when a review that included Paul Nugent of Dr. Shaw's group determined that the high-resolution of the LCAM filters were ill-suited to agriculture spectral imaging applications. Now, we want to develop an instrument that uses LCAM units to measure the spectral signal of the sun and atmospheric absorption in the atmosphere using from the sun as an illumination source.

a) As mentioned previously, we use laser ablation to produce the curved mirrors for the arrayed micro-cavities. We are modifying the system by adding an acousto-optical modulator(AOM), a diffractive optical element and some extra mirrors for better control over the laser pulse. The AOM gives us better control over the pulse length. This is important, because we need to control the amount of energy per pulse if we want to consistently produce similar craters. An inexpensive AOM and controller was purchased off Ebay. We expect to have it installed an operational within a couple weeks.

To date, almost all of the micro-cavities we have fabricated and tested contain undesirable transverse optical modes. One could argue that these modes effect the LCAM signal-to-noise ratio. A technique for minimizing the transverse modes is to increase the radius of curvature of the ablated curved mirror surfaces. To achieve this, we are going to introduce a diffractive optical element (DOE) into the system, which changes the laser pulse profile from Gaussian to top-hat profile. We have worked closely with Laser Components, which is a company that manufactures and sells DOEs. A DOE has been purchased, which will provide a 30 μm diameter top-hat beam for ablation. We expect to have the DOE installed an operational within a couple weeks. Figure 5.7 contains the optical circuit for the improved ablation system.

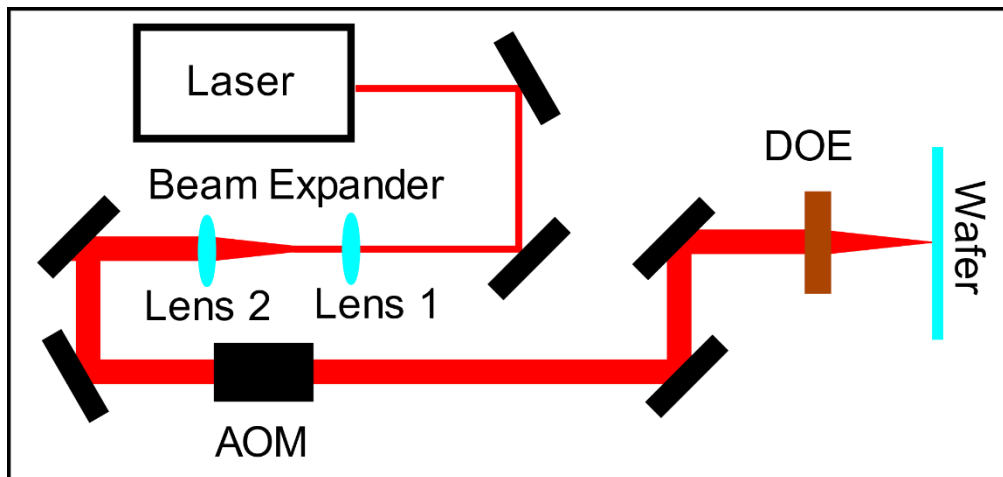


Figure 5.7 Optical circuit for the new ablation fabrication system. First, the CO₂ laser beam is expanded from 2.5 mm to 10 mm in diameter. The beam then passes through an AOM, which gives the operator control over the pulse length and laser power deposited into the wafer substrate. Lastly, a diffractive optical element reshapes the beam from a TEM₀₀ Gaussian mode to a top-hat beam profile and focuses the beam for ablation of the fused silica wafer.

b) One of the wonderful things about working with the LCAM technology is the variety of applications. For this effort, we decided to investigate the use of LCAM units for atmospheric monitoring. The general idea is that the Sun is a very bright light source and it should be simple to gather its light and filter the light with an LCAM. Various chemicals and elements in the solar and earth atmosphere absorb solar light.

Our hope is to be able to look for these spectral absorption signatures. Illustrated in Figure 5.8 is the instrument we are working on and a picture of the first prototype. A 1" fiber coupler is used to gather solar radiation and couple it to a single mode optical fiber. The light from the fiber is collimated and incident on a 45-degree mirror with the same high reflective coating as the LCAM. The purpose of this is to filter out solar light not within the band of the LCAM. The light is then focused and couple into the LCAM. After the LCAM, the filtered light is coupled to an optical fiber where it can be transported to a variety of optical detectors.

We have built a prototype instrument, which is pictured in Figure 5.8. We hope to have a few consecutive sunny days soon to test it. The primary atmospheric elements we will initially look for are water and NO_x.

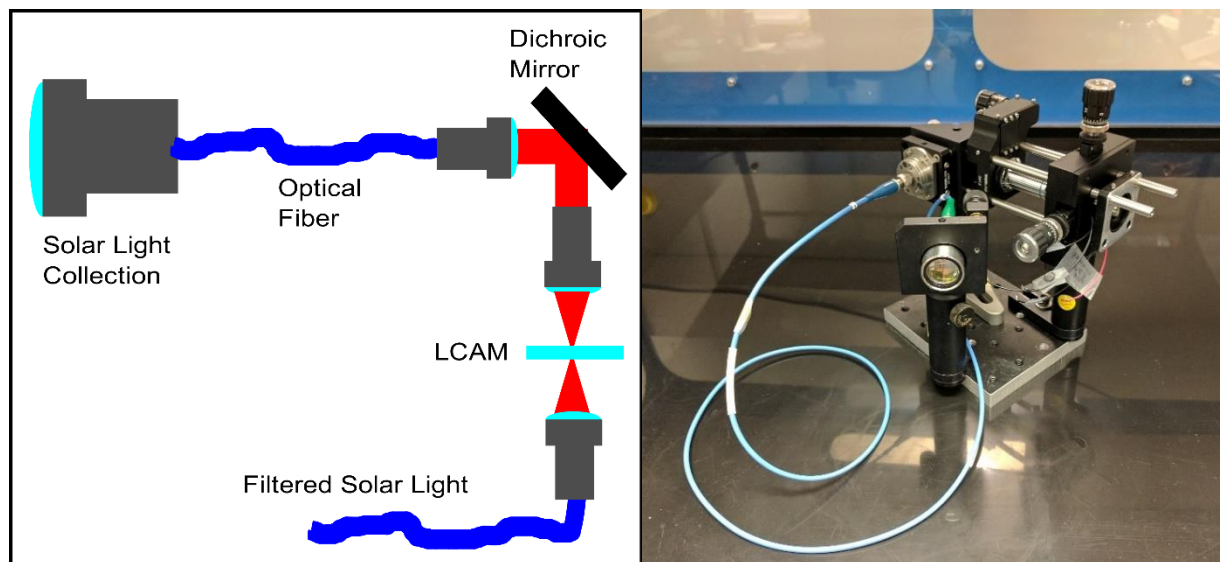


Figure 5.8 (Left) System for atmospheric monitoring with LCAM units. (Right) Photograph of the first atmospheric monitoring instrument with an LCAM unit.

c) No progress

Expenditures to date (Grant 41W418) Personnel \$61,561.22, Benefits \$22,143.70, Operation \$6,684.06;
Total Expenditures **\$90,388.98**

Subproject 6: Hyperspectral imaging for monitoring cell growth (Ed Dratz with Resonon, Inc.). Design a hyperspectral imaging system for monitoring the metabolic state of live cells in culture. Applications to stem cells for understanding disease mechanisms in individuals, drug testing in cells from individuals, potentially optimize personal nutrition, and solve Montanan's health problems.

Milestones

- a) February 1, 2016: Complete design and testing of proof-of-principle prototype hyperspectral imager with improved cost/benefit, prototype interface for cell hyperspectral analysis, and development of stem cell labeling.
- b) May 1, 2016: Integrate the prototype systems for advanced analysis of stem cell metabolism with hardware and software control. Test for evaluation of optimization of selected nutrients.
- c) October 1, 2016: Refine and improve software and operating conditions of real time hardware and software for variations of metabolic state for culture optimization.
- d) February 1, 2017: Enhance user interface to control system and software to control and optimize nutrient composition; evaluate possible changes in microscope system for improved performance.
- e) June 30, 2017: Proof of principle for feedback control of nutrient optimization with nutrient dosing control system. Investigate biochemical individuality in pilot experiment.
- f) June 30, 2017: Submit grant proposals to leverage additional support. Final report to MUS that summarizes accomplishments and commercial potential.

Activities to date

Excellent progress has been made on the various components needed to complete this project. The hyperspectral microscope system, the high speed and high accuracy sample stage, the microfluidic nutrient dosing and live cell growth chamber system, the control and analysis software, and the integration and testing of the fluorescent sensors of the metabolic state of the human adult stem cells are all progressing well.

We have submitted one grant proposal and are developing a second proposal to continue development and to move on to commercialization of the hyperspectral live cell microscope system. The first proposal has been submitted to the Montana Board of Research and Commercialization of Technology (MBRCT), with earliest possible award date of July 1, 2017. The second proposal is in preparation for the National Institutes of Health (NIH) Science and Technology Transfer (STTR) program planned for submission by June 5, 2017. The STTR and SBIR are also known as *America's Seed Fund*, and are one of the largest sources of early-stage capital for technology commercialization in the United States

Excellent progress has been made in the crucial areas of software development for instrument control and data analysis in collaboration with Dr. Snider's hyperspectral project. The Matlab software is completed to control both the Onix cell growth and microfluidic nutrient dosing system. Control of the high performance, rapid scanning and high accuracy microscope stage is the current focus of software development. A Basler camera is mounted on the stage to monitor sample images. Area scan photos from the Basler are being used for initial development. Electronic control of the stage is mostly automated and an autofocus algorithm has been tested and sets of images taken. The next step is to use the Basler camera to develop the ability to zoom in on regions of interests, picked from a low magnification image. Then development will be needed to integrate the hyperspectral line scan camera

into the system. Finally processing the hyperspectral images and a graphical user interface (GUI) will be developed.

A new high-stability optical table is soon to be installed at Montana State University to receive the microscope from Resonon. Installing the microscope in the labs at MSU will ensure the most rapid development and testing of new and improved capabilities. A single microscope vendor, Applied Scientific Instrumentation (ASI), was able to provide a high-performance inverted microscope component, which has a very open design for optical access and is also extremely stable. The ASI Modular Infinity Microscope is clearly the best solution as a optical framework system for this project. This vendor is the only US manufacturer of integrated microscope systems and will provide the best possible price on the complete optical systems needed for development of a commercial product. This excellent price for the optical components will facilitate the commercialization of the complete hyperspectral microscope with the integrated microfluidic cell culture system and complete, powerful computer control and software system that is under development.

Prof. Snider's team has made progress with the software hyperspectral data acquisition and processing software and have largely integrated the software to control the automated XY sample stage, which has to be able to scan in small, very high resolution steps for maximum hyperspectral resolution, along with rapid movement speed (7mm/sec in this case), so we can rapidly revisit cells in the field for repeated spectral measurements after modifying the nutritional state.

Continuing progress has been made in the Dratz lab on introducing optogenetic probes of the oxidation/reduction state into human adult stem cells and other useful cells in culture. The probes have been transferred to efficient carrier vectors, that are providing improved, more facile optical probe introduction. We have also introduced the optogenetic probes into murine smooth muscle cells to begin demonstrating the wide applicability of our systems for metabolic monitoring of live cells. There is a great deal of local experience with these smooth muscle cells and monitoring the control of the metabolic state if these cell lines. A graduate student in the Dratz lab is devoting full effort to working with the optogenetic probes, assisted by a research undergraduate, two postdoctorals in the Reijo Pera lab, and Robert Usselman, a Research Assistant Professor in the Singel lab, all in the MSU Chemistry and Biochemistry Department. An advanced undergraduate Electrical and Computer Engineering (ECE) Design Team in the Snider lab in Electrical and Computer Engineering has completed the controller for the cell culture environmental control system, as noted above and is continuing to design the microscope stage controller system, which can make much faster progress now that the fast and accurate stage is installed. A graduate student in the Snider lab is devoting full effort to the high-speed hyperspectral imaging analysis software and will be working on this crucial aspect of this project into the next year. The personnel include two graduate students devoting full effort to the project, two advanced undergraduates on an ECE Design team.

Software activities in the Snider Lab

The names and length of the function names are intuitive for the operation to be performed. Some usability was also added. For instance the AcitveX command to open well groups on the CellASIC is `onix.OpenWellGroups("00X00X00")`. Where `nix` is the object created by the `actxserver` command, and `"00X00X00"` corresponds to well groups 1 through 8 from left to right. This is a cumbersome way of telling the CellASIC to open wells 3 and 6 to pressure X. It also doesn't provide an easy way to set the pressure. Using the Matlab command for this same action is done by: `OpenWells([3 6], 2)`. Here '[3 6]'

are the well groups to open, and '2' is the pressure in kPa at which to open them. Two separate ActiveX commands are needed to do this, the one above and `onix.SetPressureX('2')`. Both of these are handled within the Matlab function `OpenWells`. A command to close the wells, `CloseWells`, has been created as well, which operates similar to the `OpenWells`, but without the pressure argument.

Other functions set the temperature and add time between commands providing the ability to perform most CellASIC experiments through a Matlab script file. Future work will allow for as much control as the ONIX2 software provides, including the ability to have dual pressures, and sending emails if an error occurs. Below is an example Matlab script that controls the CellASIC platform.

```
global onix; onix = actxserver('ONIXCOMServer.OnixHandler');
Temperature(37.5) %set temp to 37.5C
OpenWells([6],1.8) %open well 6 and load cells
WaitTime(0,0,6) %0hours 0mins 6sec
OpenWells([2],4) %open well 2 with 4kPa and close well 6
WaitTime(8,0,0) %8hours, 0mins, 0sec
OpenWells([3],4) %open well 3 with 4kPa and close well 2
WaitTime(8,0,0) %8hours, 0mins, 0sec
```

The ASI Company, in Portland, has also expressed interest in teaming with us to refine the development of our planned commercial product. The microscope will do an initial rapid scan of the image field, the software will locate cells, and the cells will then be scanned at high resolution repeatedly during the course of the experiments. Thus, the stage has to be able to scan rapidly between cells and then switch to much slower, small step sizes for high- resolution imaging. The software control for the XY stage and Z automatic focusing with programmable nose piece for changing objectives for different magnifications is in prototype and will be tested as soon as the stage arrives.

Expenditures to date (Grant 41W414) Personnel \$55,322.94, Benefits \$9,024.50, Operations \$46,809.05, Capital Equipment \$74,502.70; total Expenditures **\$185,659.19**.

Subproject 7: Translational research to commercialize micro-mirror technology (Arrasmith at Revibro Optics). Translate MSU-developed deformable mirror technology to a commercially sustainable product.

Milestones

- a) June 30, 2016: Refine production to achieve a repeatable fabrication process. This milestone will involve a redesign of fabrication masks, purchase of new wafer bonding equipment, and refinement of wafer bonding process
- b) Obtain funding from another source. Revibro will pursue funding through commercial sales and commercial R&D efforts (June 2016), and through SBIR/STTR or similar government funding (June 2017)
- c) Create 2 full time Montana jobs: One job will be created immediately to sustain the founder of Revibro – August 2015; Technical and/or sales and marketing hire – December 2015

Activities during Q6

- Completed construction of a new wafer bond aligner
- Improved device yield from 10% to > 50% by improving fabrication procedures
- Pursued commercialization efforts

During Q7 Revibro continued to support our first two customers, who purchased prototype mirrors early in 2017. Since this is a new technology, we expect to keep support relationships open with these two early adopters. It will also be very beneficial for us to get valuable feedback of our products and technology from early adopters. We are very pleased to have solid commercial revenue for the first time in 2017.

Related to Milestone A, during Q7 Revibro designed and built a wafer alignment system for use in the Montana Manufacturing Facility (shown in Figure 6.1). Our fabrication process relies on a bonded wafer approach where a bottom “electrode” wafer is aligned to and bonded with a top “mirror” wafer. Previously a single camera was used to perform this alignment by capturing an image of the entire wafer surface. This new alignment system uses two cameras, allowing each camera to zoom in on much smaller alignment features for higher precision. The old system had a field of view of ~5 inches, while each camera on the new system has a field of view of ~1/16”. Using this new aligner, we have produced bonded wafers with much higher tolerance, resulting in a release aperture that is centered properly on the deformable mirror surface. In conjunction with design and assembly of the new aligner, we designed software to show both images simultaneously, and allow the user to capture a snapshot of the bottom wafer then overlay the live video feed from the top wafer for alignment. Figure 6.2 is a screen capture from the aligner software.

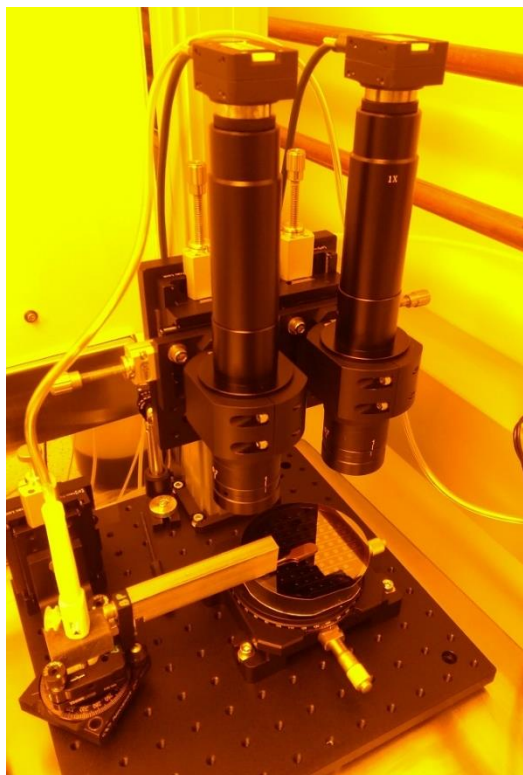


Figure 6.1. Custom-built wafer alignment system.

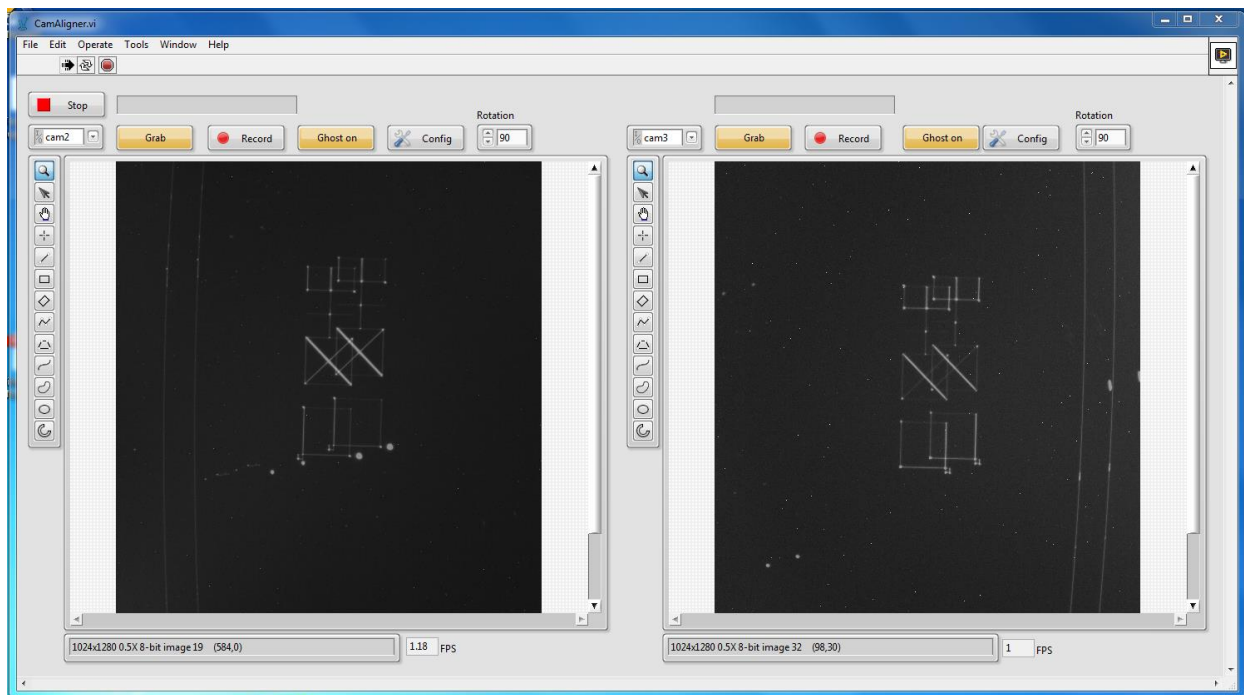


Figure 6.2. Screen capture from aligner software.

Also in Q7, we developed a new material stack for spacing the electrodes and mirror surface at a uniform distance across the wafer. Historically the yield of optically flat mirrors from a wafer (each wafer has 60 mirrors) was very low, around 10% (or 6 mirrors). Using this new spacer layer material and procedure, we have produced two wafers with more than 50% flatness yield. This results in a 5x reduction of device cost, and gives us confidence that we can repeatedly produce high-quality mirrors to meet future customer demand.

We have also been actively pursuing commercialization efforts. Revibro is happy to have received a Phase I SBIR grant in February 2017. In order to successfully pursue a Phase II grant, we need to develop a robust commercialization strategy for our technology. To that end, we have conducted more than 40 interviews with potential customers, end users, and other players in the supply chain. During the next several months we will continue to talk to people in the microscopy industry to ensure our technological developments are synergistic with market needs, and to refine our commercialization strategy and business model.

Total Expenditures: (Grant 41W410 Sub-Award) Personnel & Benefits \$205,208.79, Total Expenditures **\$205,208.79.**

Subproject 8: Active waveguides and integrated optical circuits (Rufus Cone, collaborating with Babbitt, Nakagawa, Barber, Himmer, Avci, and Thiel with S2 Corp., AdvR, FLIR/Scientific Materials, and Montana Instruments).

Our goal is to advance and integrate unique Montana technologies, expertise, and capabilities to improve marketability, performance, and enable additional Montana photonic products. These optical, or “photonic,” devices can provide performance far beyond the capabilities of modern electronics. Our MREDI work develops new capabilities and technologies at MSU directly targeted at increasing Montana participation in international markets that use light “guided” through crystals to process information. These integrated photonic “waveguide” devices have many more functionalities than the more familiar optical fibers and are the essential next generation of product applications. The word “integrated” here implies subminiaturized packaging of the type familiar from modern electronics. Indeed, we are making “circuits for light.”

Our vision is to employ special rare-earth-activated crystals produced by Scientific Materials-FLIR with the waveguide design and the miniature packaging capabilities of AdvR Inc., all integrated with Montana Instruments Corp. low-temperature systems to enable photonic signal processing systems produced by S2 Corp., leading to new products for each company. This project involves broad interdisciplinary collaborations between six different research groups at MSU from several departments and centers, all working with the four local Montana companies above, providing unique synergy that establishes a long-term program of sustainable collaboration in this field, with short-term development focused on immediate return for Montana businesses and current research programs at MSU. *This collaborative, Montana-focused effort is only made possible by the MREDI program, opening completely new opportunities to leverage unique Montana technologies towards research and development efforts that are beyond the capabilities of individual research groups or companies.*

Milestones

- a) Fall 2015: Fabrication of rare earth doped optical waveguide suitable for optical signal processing applications (SUCCESS)
- b) Summer 2016: Integration of an optical waveguide into a cryostat (SUCCESS)
- c) Spring 2017: Demonstration of SSH processing in a cryogenic waveguide (In Progress)
- d) June 2017: Final report summarizing technical results and emphasizing commercial potential (In Progress)

Activities during Quarter 7

During this seventh reporting period, coordinated research and development activities continued to achieve our final objectives in close collaboration with our Montana industrial partners. Work is on schedule for demonstrations of photonic signal processing in cryogenic waveguides. Below, we outline some of our new results during this quarter regarding the economic, scientific, and educational successes and impacts of our MREDI supported efforts.

New impacts on Montana student education and training:

The MREDI effort has provided a unique educational opportunity for Montanans at all levels of education. Undergraduate and graduate students continue to work in close collaboration with professionals in the local optics industry, with benefits for all involved. As a recent example, graduate student Tino Woodburn has been working directly with Scientific Materials Corp. in Bozeman on methods to reduce thermal gradients in the crystal growth process, enabling new materials to be produced for scientific study at MSU and commercial products, providing practical real-world educational experience, and expanding the production capabilities of our local Montana industry.

During this quarter, three undergraduate students working on our MREDI effort wrote and submitted successful summer research proposals to the MUS Undergraduate Scholar's Program. John Pommer was awarded a grant for his project proposal *"Design and Implementation of an Apparatus to study Magnetic Anisotropy of Rare-earth-doped Crystals at Cryogenic Temperatures."* Riley Nerem was awarded a grant for his project proposal *"Raman Echo Spectroscopy of Rare-earths Using Dual Frequency and Phase Locked Lasers."* Jason Carr was awarded a grant for his project proposal *"Chemical Processing of Lithium Niobate Crystals for Improved Optical Properties."* All three of these projects build directly from the experience that they gained while working on our MREDI-supported research.

Undergraduate students Kyle Olson and Riley Nerem presented posters on their MREDI-supported research during the annual Student Research Celebration on April 21, 2017. Kyle's presentation was on *"Rare-Earth-Doped Waveguide Development and Characterization"* (Figure 8.1) and Riley's presentation was on *"Scanning Fabry-Perot Interferometers for High-resolution Laser Systems."*

Graduate student Tino Woodburn volunteered at the 3rd Annual STEAM Night at the Hawthorne Elementary School in Bozeman on Jan 26th, and he volunteered for two days at the Lone Mountain Mind Benders preschool during this quarter to encourage interest in science and technology.

Research Engineer Tia Sharpe of Spectrum Lab received training and experience in the Montana Microfabrication Facility on the e-beam evaporation deposition system during this quarter. Tia also received new training on handling the acidic chemicals used for developing photolithographic resists.

Also during this quarter, Prof. Rufus Cone hosted undergraduate students Micah Johnson, Sam Liebersbach, Rowen Oswald, Mikaela Barker, and Brady Griffith, providing an overview lecture on our MREDI-supported research, discussion of research opportunities for students at MSU, and giving a tour of the laboratory facilities on April 13, 2017.

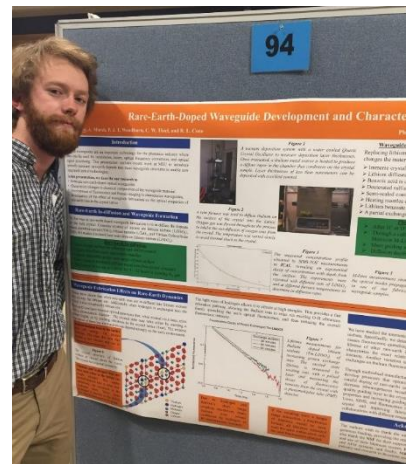


Figure 8.9. Undergraduate student Kyle Olson presented a poster on his MREDI-supported research into "Rare-Earth-Doped Waveguide Development and Characterization" at the annual student research celebration.

New impacts on University research funding:

This MREDI project has already had a significant impact on new research funding at Montana State University, as highlighted in detail in the previous quarter's report. Our work continues to nurture new ideas in their early stages, provide new experimental and computational capabilities, generate new ideas from interdisciplinary collaborations, and illuminate opportunities for new technologies from interactions with the local Montana optics industry.

During this quarter, Spectrum Lab began work on a new subcontract from S2 Corporation. This subcontract includes \$148,000 of funding for two years (2017 – 2019) as part of an NSF Phase IIB SBIR project. The goal of this project is to develop a compact optical system to couple to the bulk S2 crystals for S2-Spectrum Analyzer and S2 processor applications. This project benefits from our next milestone and is directly relevant to the MREDI Active Waveguides subproject.

New impacts on Montana university competitiveness:

MREDI continues to have a significant positive impact on the educational and scientific competitiveness of the Montana University System. During this quarter, several new experimental and diagnostic capabilities were implemented. Undergraduate student Riley Nerem completed construction and testing of a scanning Fabry-Perot interferometer system to characterize lasers needed to probe Cr³⁺ ions in crystals and began construction of a second system to characterize Yb³⁺ ions in crystals required for our collaborative research efforts with California Institute of Technology. These systems will also be a critical enabling component of Riley's summer research project supported in part by the Undergraduate Scholars Program.

Work continued on expanding our Montana Instruments Cryostation system, including design and construction of a range of new cryogenic sample holders as well as implementation of new window housings incorporating optical windows with anti-reflection coatings matched to laser wavelengths used with our rare-earth-activated waveguides.

During this quarter, a new high-sensitivity InAs photodiode infrared detector was incorporated into our optical spectrometer to enable direct study of hydrogen impurities in crystals. These measurements are required to study crystal composition and structural phases when fabricating waveguides by chemical proton-exchange methods. That system will also provide a key resource for local company AdvR, Inc to help optimize their waveguide fabrication process for nonlinear frequency conversion applications.

Optical crystal cutting, grinding, and polishing capabilities at MSU were also significantly expanded during this quarter. A mechanical stage and feed system was designed and built to enable waveguide wafer dicing using an existing low-speed diamond saw at MSU. A flexible stereo microscope inspection system was also integrated with our precision tungsten wire saw to allow close inspection while extremely thin crystal wafers are fabricated. In addition, a faceting system was set up to allow crystal samples with complex shapes and orientations to be readily and reliably fabricated.

New impacts on Montana industry competitiveness:

Our MREDI efforts have a range of broader impacts on the local optics industry. We have worked closely with Scientific Materials Corp. to develop a crucible after-heater design that reduces thermal gradients and crystal strain during crystal growth. This effort was led by MSU materials science graduate student Tino Woodburn and successfully enabled larger single crystals of the important optoelectronic crystal lithium niobate to be produced. Using this approach, Scientific Materials Corp. grew a new lithium niobate crystal (shown in Figure 8.2) that incorporates thulium ions for photonic signal processing at S2 as well as magnesium ions that increase the optical damage threshold of the material. Additional growths of lithium niobate and lithium tantalate crystals are underway. These new materials are vitally important to research efforts at MSU and to photonic signal processing applications at S2 Corporation. They are also of broader commercial interest as a product for Scientific Materials Corp., with inquiries by international customers regarding these materials already being received.

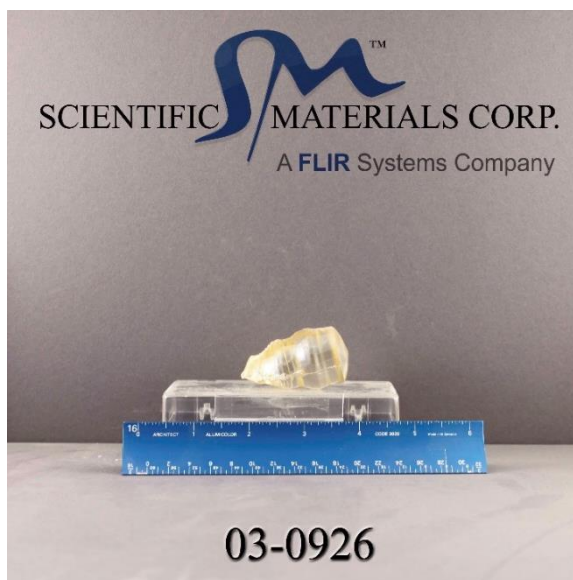


Figure 8.10. A new single crystal boule of lithium niobate doped with thulium and magnesium ions was grown by Scientific Materials Corp. with assistance from MSU researchers and students as part of our MREDI effort.

We have continued to work with AdvR Inc. on a variety of commercially important research topics. In addition to the work developing new waveguide characterization methods discussed in detail later in this report, we have also continued to study the effects of hydrogen impurities used by AdvR Inc. to produce optical waveguides in lithium niobate crystals. We are also assisting AdvR Inc. to characterize their laser sources using an optical delayed self-heterodyne system constructed at MSU.

Our innovations and studies all directly impact the photonic signal processing devices under development at S2 Corporation. As one example, Figure 8.3 shows a crystal grown by Scientific Materials Corp. that we engineered to have a significantly increased optical signal processing speed; in the Figure it is being studied at MSU using a Montana Instruments cryocooler.

International scientific collaborations:

During this quarter, several researchers have visited MSU to discuss our MREDI-supported efforts and to develop or enhance ongoing scientific collaborations. Most recently, postdoctoral research John Bartholomew and doctoral student Jon Kindem from Prof. Andrei Faraon's Nanoscale and Quantum Optics Research Group at California Institute of Technology visited MSU for experiments during April 24-

30, 2017. During that visit, new optical materials were characterized for potential nanophotonic and quantum information device applications. All travel expenses for this collaborative effort were paid by California Institute of Technology; this demonstrates the importance and capabilities of our laboratory, which in this area exceed those available at Caltech. Visits to MSU by international researchers have been scheduled, with Dr. Lucile Veissier from Laboratoire Aimé Cotton in Orsay, France, planning to visit MSU May 7 to 22, 2017, and doctoral student Sacha Welinski from Laboratoire de Chimie de la Matière Condensée de Paris in Paris, France, planning to visit MSU May 22 to June 22. All travel expenses will be paid by their respective research institutions.

Several prominent scientists and researchers visiting MSU presented colloquium talks in addition to discussing our research projects. On February 22, Dr. Tian Zhong from California Institute of Technology presented a colloquium on “Building a quantum internet using rare-earth-doped crystals.” On March 31, Dr. Mark B. Ritter, Distinguished Research Staff Member at IBM Research in Yorktown Heights, NY presented an MSU colloquium on “Quantum Simulation with Circuit Quantum Electrodynamics” as well as a public lecture at the Museum of the Rockies on “The Future of Computation.” On April 21, Dr. Jun Ye, Fellow of JILA and Fellow of NIST from the University of Colorado presented a colloquium on “Atomic clock and quantum matter.”

New impacts on international promotion of Montana science and industry:

Our MREDI research efforts continue to increase the exposure of the local optics industry to international markets. One activity toward this goal is the recent work by researchers and students in Rufus Cone’s group on developing an exhibit for the American Computer Museum in Bozeman (www.compustory.com) to highlight the unique signal processing and quantum information research and industry present here in Montana. This public display will explain to the broader public how the technologies being developed and commercialized here in Montana will enable the next generation of computing and communications.

We have also been working with Evangeline Koonce (Figure 8.4), a student in the Montana State University Master of Fine Arts in Science and Natural History Filmmaking (SNHF) program, to make short videos about the optics research and technology in Montana. In addition to short videos, a series of 90-second podcasts about science are also being produced. An additional project has been approved to continue this collaboration during summer 2017.

During this quarter the Cone research group also received a significant honor by one of their scientific publications on materials for optical

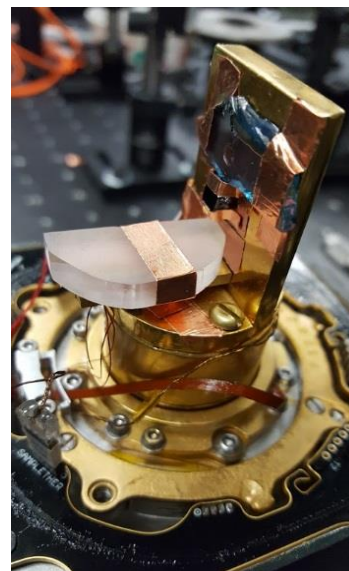


Figure 8.11. A single crystal of Er:YLuAG grown by Scientific Materials Corp. is mounted in a Montana Instruments Cryostat for study at MSU, where its properties are evaluated for the photonic signal processing products developed by S2 Corporation.



Figure 8.12. MSU filmmaking graduate student Evangeline Koonce is working with MREDI students to produce educational videos about optics research in Montana.

signal processing and quantum information being included in a special issue of the Journal of Luminescence entitled “Luminescence Legacy” (www.journals.elsevier.com/journal-of-luminescence/virtual-special-issues/luminescence-legacy). This MSU research publication was one of only 15 chosen for this special issue; it was selected from more than 13,000 peer-reviewed publications spanning the 47-year history of the international journal.

New scientific research publications:

During this quarter, two papers describing parts of our MREDI-supported research were published in peer-reviewed scientific journals.

- “Enhanced properties of a rare-earth-ion-doped waveguide at sub-Kelvin temperatures for quantum signal processing,” N. Sinclair, D. Oblak, C. W. Thiel, R. L. Cone, and W. Tittel, *Physical Review Letters* 118 (2017) 100504.
- “Effects of mechanical processing and annealing on optical coherence properties of Er³⁺:LiNbO₃ powders,” T. Lutz, L. Veissier, C. W. Thiel, P. J. T. Woodburn, R. L. Cone, P. E. Barclay, and W. Tittel, *Journal of Luminescence*, In Press, available online (2017) doi: 10.1016/j.jlumin.2017.03.027.

Additional technical highlights of recent project activities (Q7):

Study of Thulium-doped YAG Bulk Crystals and Planar Waveguides

During this quarter, we have begun to investigate the potential for general waveguide fabrication in traditional bulk optical signal processing materials such as thulium-doped yttrium aluminum garnet (YAG) used in MSU Spectrum Lab and S2 Corporation devices. Specifically, we are examining high-energy ion-implantation methods and determining whether structural damage caused by ion bombardment affects the resonant optical properties and relaxation dynamics. While this method of waveguide fabrication is very general and can in principle be applied to a wide range of optical crystals, it is also one of the most damaging to the crystal due to both the high kinetic energy of the implanted ions as well as the changes in chemical composition from addition of the ions and potential vaporization of the more reactive lattice constituents such as oxygen.

A microscope image of the edge of a planar optical waveguide fabricated in a Tm:YAG optical signal processing crystal that we are studying is shown in Figure 8.5. The waveguide has a thickness of 6 microns to provide single transverse mode propagation at 793 nm. A clear brown coloration in the guiding regions is apparent, indicating the presence of a broadband optical absorption induced by the ion-implantation process. This absorption likely indicates the presence of oxygen vacancies, suggesting that the ion implantation process imparts enough energy to cause oxygen to be ejected from the crystal lattice. We expect that this detrimental effect can be partially reversed by high-temperature processing in an oxygen-rich atmosphere to enable oxygen ions to diffuse back into the vacancies in the lattice. We also found that the waveguide region is very susceptible

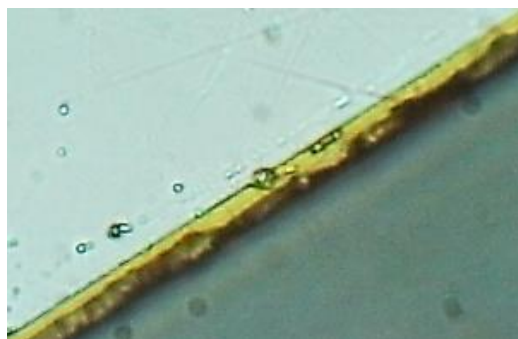


Figure 8.13. This microscope image of the edge of a planar optical waveguide in a Tm:YAG photonic signal processing crystal shows damage due to mechanical polishing and discoloration likely caused by a change in chemical composition in the guiding region.

to physical damage, as seen by the chips observed in Figure 8.5, perhaps indicating that the implanted region is mechanically weakened by the damage caused to the crystal lattice. It is unknown to what degree this structural damage can be reversed or “healed” by thermal and chemical processing without adversely affecting the guiding properties.

Initial studies of temperature dependence and spectral hole burning were carried out on the Tm:YAG waveguide sample, with a typical spectral hole burning measurement shown in the oscilloscope trace in Figure 8.6. The change in material transmission (i.e. spectral information stored in the crystal) is indicated by the sharp transmission feature, or “spectral hole”, in the lower trace. Analysis and additional measurements are evaluating how waveguide fabrication affects the spectral hole burning dynamics that determine material performance in photonic signal processing applications such as those developed by MSU Spectrum Lab and S2 Corporation.

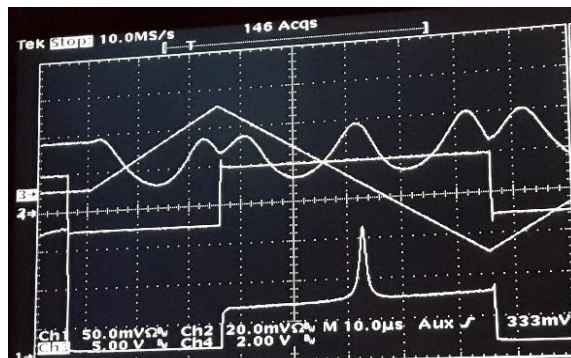


Figure 8.14. This example of experimental data shows spectral hole burning in a thulium doped signal processing crystal that contains a planar waveguide.

Fluorescence microscopy of rare-earth-doped crystals:

Work has continued on developing and improving our capabilities for fluorescence and Raman microscopy of waveguide structures. Fluorescence images of rare-earth-activated samples have been obtained, but the optically tunable filters are not yet properly synchronizing so the detection sensitivity is lower than it should be. Undergraduate student Kyle Olson is investigating the source of this problem, whether from the hardware or the software, and determining if it can be readily corrected. In the current configuration, the system allows detailed fluorescence images to be acquired, achieving our primary goal, but has a reduced capability for capturing full spectrally resolved spectra required to perform more detailed chemical and structural analysis of the samples.

Study of Proton and Deuterium Exchanged Waveguides

New thulium-doped LiNbO₃ planar waveguide samples have been fabricated using both proton exchange and deuterium indiffusion. Samples produced using different exchange times were studied by time resolved and spectrally resolved fluorescence studies of the thulium ions. These studies further support our model for the proton-induced relaxation dynamics as being only a very short range interaction, allowing some fraction of the incorporated thulium ions to be unaffected by the fabrication. Further studies are in progress to determine how the proton exchange process affects other optical transitions for thulium and other rare-earth ions such as erbium used for operation in the 1.5 micron telecommunications band).

Study of optical coupling to rare-earth-activated waveguides:

Due to the critical importance of the shape and size of optical beams in determining how they couple into the very small micron-sized waveguides in crystals, we have explored a range of approaches for interfacing input laser light with the waveguides. Lenses with longer focal length lenses than those commonly used are required to interface with the Montana Instruments cryostation; the longer focal lengths make it

challenging to achieve good coupling efficiency, but they allow much greater flexibility in the optical system design. The performance of varied lens systems, balancing geometrical aberrations and diffraction effects, has enabled very small focused laser spot sizes. Using an arrangement such as shown in Figure 7, light from a single mode optical fiber was collected and focused onto laser beam profilers and onto the optical waveguides to characterize performance. Combinations of achromatic doublet and triplet lenses were purchased and tested by postdoctoral researcher Caroline Richard, who is shown in Figure 8.8; configurations were found that produce as little as 2 microns of additional broadening (i.e. blurring) relative to the theoretically limited spot size. Consequently, we have established that these lens systems produce sufficiently small spot sizes that efficiently couple into the ~6 micron sized single mode crystal waveguides at the 795nm thulium wavelength, while also providing focal lengths that are long enough to allow free-space coupling into the Montana Instruments Cryostat system using lenses located outside of the cryostat. This significantly simplifies the system design and adds flexibility.

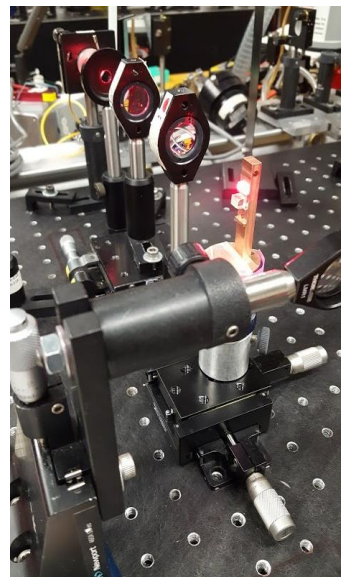


Figure 15. Experiments study the effects of laser beam quality and optical component selection on coupling of light to waveguides.

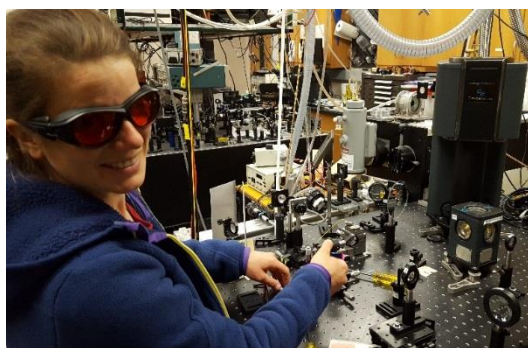


Figure 8.16. Postdoctoral researcher Dr. Caroline Richard is investigating laser focusing and spot sizes for coupling light into waveguides in the Montana Instruments Cryostat system.

To further increase waveguide coupling efficiency and expand our spectroscopic capabilities, we have also purchased and installed a selection of new cryostat windows with anti-reflection coatings matched to different rare-earth transition wavelengths. These windows reduce the optical power lost to reflections and also eliminate undesired interference effects from multiple reflections within the windows.

Fabrication and modeling of nano-scale periodically poled nonlinear crystals

This last quarter we continued our efforts, in collaboration with a Montana Space Grant Consortium (MSGC) funded project, to develop optical waveguide devices for performing wavelength conversion under novel conditions. One application is the highly sensitive conversion and detection of low photon number signals. In fall 2016, initial poling tests were performed and had a promising degree of success. However, higher fidelity transfer of poling electrode width to final poled domain width was required. A second lithographic mask was developed that will allow fabricating electrodes of varying electrode duty cycle to improve poled domain width for various grating periods. Poling tests on lithium niobate using the electrodes developed with this new mask were conducted with industrial collaborator AdvR, Inc. A microscope image of a portion of one of these electrodes is shown in Figure 8.17. This new set of electrodes was used to pole a lithium niobate crystal. Characterization of the achieved domain widths, using our new piezo-response force microscopy capabilities developed under MSGC funding, showed results much closer to 50/50 domain duty cycle than with previous poling tests.

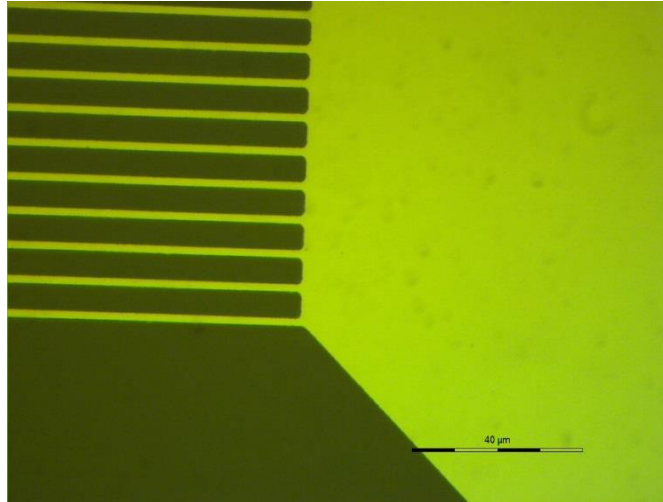


Figure 8.17. Optical microscope image of improved chrome micro-scale periodic grating electrode structure for poling ferroelectric crystals. Grating period is 8 microns. Electrode width is 2 microns.

To continuously improve fabrication of micron and nano-scale poling electrodes for non-linear optical crystals, a student was trained on the Image and Chemical Analysis Laboratory's (ICAL) field emission scanning electron microscope (FE-SEM). This has allowed better investigation of the quality of electrodes and informed us of 100-200 nm defects in the form of edge roughness in our chromium thin film deposition process for the poling electrodes. Methods and deposition rates were investigated for making the chromium thin films on insulating silica wafers. Montana Microfabrication Facility's (MMF) sputter and physical vapor deposition (PVD) systems were used, and the wafers were diced by collaborator AdvR Inc. Preliminary results show a reduction in the size of defects on fabricated electrodes by a factor of three using the sputter system with a deposition rate of 2 \AA/s . An FE-SEM image of the improved electrodes is shown in Figure 18. This is a promising result that is being further investigated to confirm repeatability. This reduction of defect size will have the dual effect of better domain fidelity when poling on the micron scale, and improving precision alignment when patterning nano-scale electrode structures with electron beam lithography (EBL). Work on these nano structures has also progressed. We have fabricated several nano-scale poling electrodes and improvements in EBL dosage and etch timing of final chromium layer are currently ongoing.

Another aspect of our nano-scale poling project has been to model the behavior of the electric fields involved in the complex process of inverting ferroelectric domains. This is important for understanding the physics behind our experiments and for guiding our fabrication and experimental parameters in developing improved poled devices. New development on the grating electrode model using COMSOL Multiphysics software continued during this quarter. The model's efficiency was improved dramatically by incorporating periodic domain boundaries and incorporating only a few periods of the periodic grating electrode structure instead of the full geometry. **Error! Reference source not found.** shows the high field region at the corner of an electrode, which may be critical in the initial formation of inverted domains during poling. Development of a comprehensive model to compute the electric field in a non-linear ferroelectric crystal and to simulate the field of an inverted ferroelectric domain is ongoing.

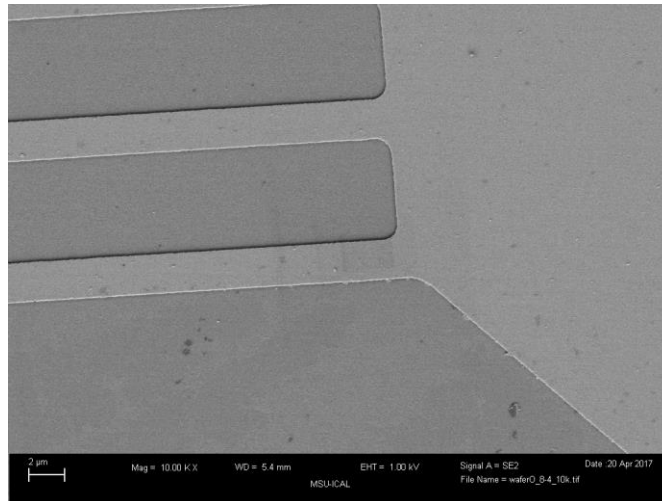


Figure 18. FE-SEM image of smoother electrode structure using sputter deposition of chromium. Grating period is 8 microns with 2-micron electrode fingers. Scale bar on lower left is 2 microns wide.

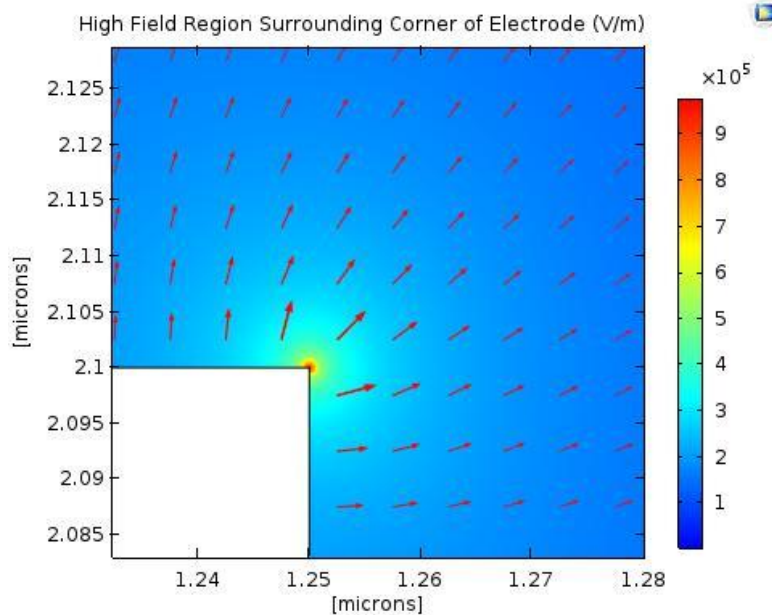


Figure 8.11. COMSOL model showing the high field region surrounding the corner of a nano-scale conducting electrode. This is thought to be a critical region for the seeding of domains during the poling process.

Testing vibrationally induced coherence loss in closed-cycle cryostats:

Over the last quarter, we continued investigations of the vibrationally induced coherence loss in a Montana-produced low vibration closed-cycle cryostat, provided by S2 Corporation. Optimal performance of spectral holographic processing devices, in waveguides and bulk, depends on achieving the long coherence times afforded by spectral spatial (S2) materials. The S2 material coherence times can be degraded due to the stresses, vibrations, or compressions introduced during the mechanical cycling of a closed-cycle cryostat. The physics behind this loss in coherence is still an open question. Developing sensitive techniques for measuring these coherence losses and their time dependence will help in the investigation of the physics of this phenomenon as well as in the design of practical cryostats for S2 signal

processing devices, such as those produced by Montana companies S2 Corporation and Montana Instruments.

This quarter we made further improvements to the experimental setup. In particular, a significant reduction in experimental noise was achieved by substituting the digital laser current driver for an analog driver, which had significantly lower current noise. Photon echo measurements with the improved system provided more conclusive statistics, with higher confidence that the effects of cryocycle vibration were not linear, but closer to quadratic, in the input pulse delay.

The photon echo energy with a fixed delay between the two input pulses, τ_{21} , was measured as a function of the experiments delay within the cryocycle, t_{cryo} . These measurements were conducted to determine the t_{cryo} delays at which the vibration-reduced broadening was maximized and minimized (Figure 8.19). These cryocycle delays were used in the second set of measurements to compare coherence loss during and away from cryocycle pulses.

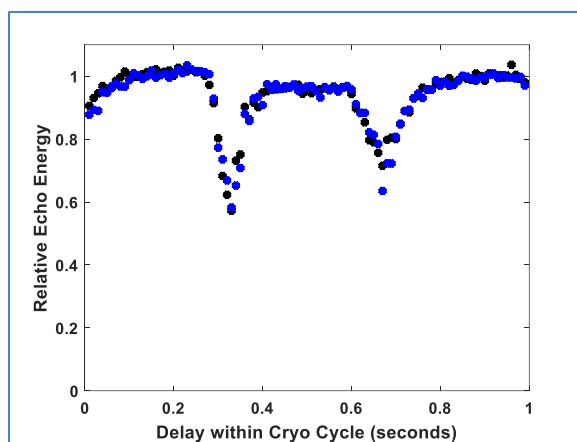


Figure 8.19. The photon echo energies measured throughout the 0.7 second cryocycle of the cryostat, normalized to have an average peak value of one. They show that maximum echo energy loss, and thus maximum broadening, occurs at t_{cryo} of about 335 and 675 milliseconds. The minimum broadening happened around 180 milliseconds, and this cryo delay was used as the reference for non-cryostat pulsing related coherence decay in the next set of measurements.

The second set of measurements also employed the two-pulse photon echo technique, where each measurement of coherence decay was done by varying the delay between input pulses τ_{21} with a fixed cryocycle delay t_{cryo} . The measurements were taken using the three cryocycle delays determined above (two “on” and one “off/reference” measurements). The method for taking the measurements were that at each τ_{21} delay, the photon echo energy was measured with t_{cryo} set for minimized broadening, then with t_{cryo} set to the delays that coincided with the two broadening maxima. To look at the coherence loss (broadening) effects associated with the cryocycle as a function of τ_{21} , we calculated the logarithm of the echo energies and subtracted the data from each broadening maxima from the data with minimized broadening (Figure 8.20). The full experiment was repeated four times to demonstrate repeatability, thus there are four sets of points per graph.

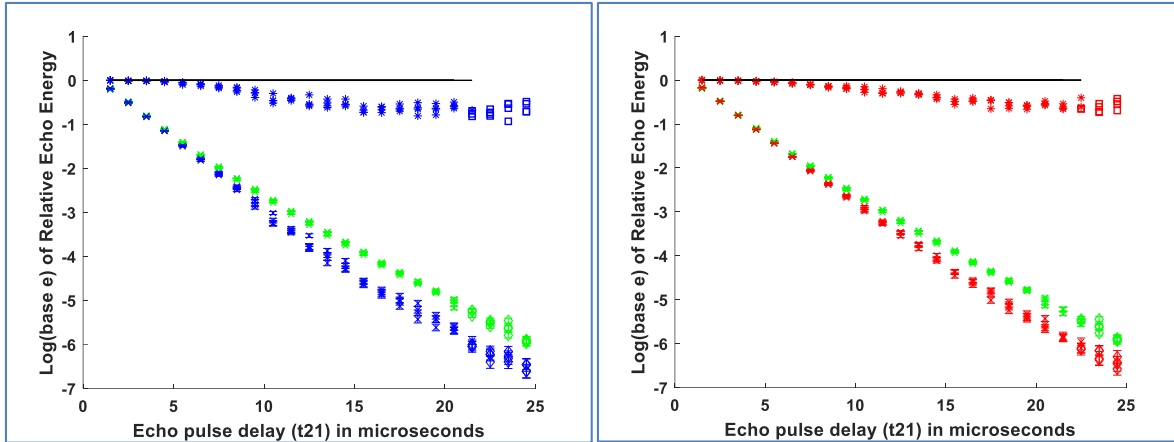


Figure 8.20. The logarithms of the normalized photon echo energies as a function of τ_{21} , measured at three cryocycle delays: one at a delay with minimal vibrational broadening (green points both plots) and two at delays with peak vibrational broadening (lower blue at left and lower red at right). The left (blue) data corresponds to the 335 millisecond delay and the right (red) data corresponds to the 675 millisecond delay. Each data point is the mean of 64 measurements of the echo energy. The standard deviation derived from these 64 measurements is shown as error bars on each data point. The upper left (blue) and upper right (red) points are the differences between the lower sets of points.

These differences between the on and off cryocycle pulse measurements were fit to determine the power law dependence of the curves. Both trends fit a quadratic trend best overall. The fits to quadratic dependence are shown in Figure 21. We are in the process of comparing these trends to various theoretical predictions to better understand the physics involved in cryocycle broadening.

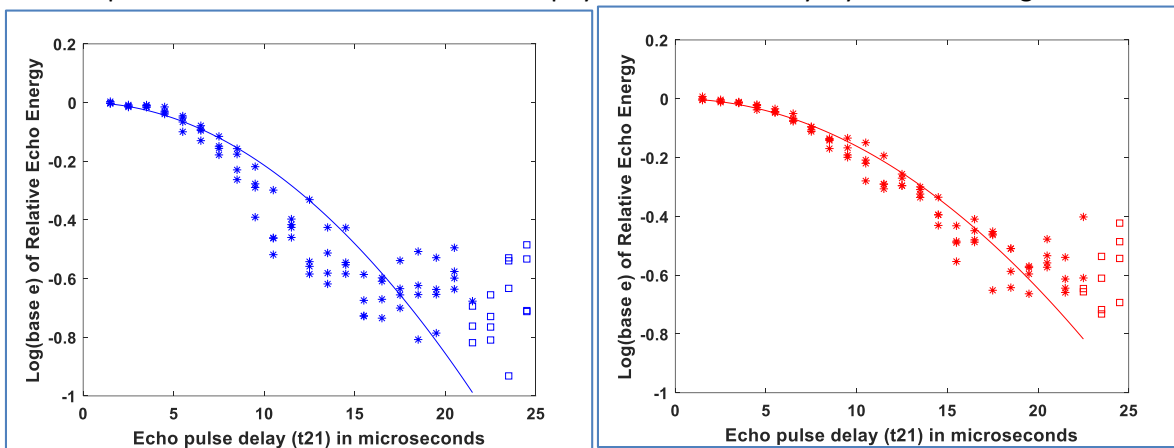


Figure 21. The logarithms of the differences of the normalized photon echo energies between measurements with maximized broadening vs. minimized broadening. The left (blue) data represent data with the maximized broadening at 335 millisecond delay and the right (red) data represent data with the maximized broadening at 675 millisecond delay. The curve represents the fit of the data, using a function of the form $a(\tau_{21})^b$. Both result in a fit that is quadratic, or $b=2$.

The understanding of cryocycle broadening will benefit future projects being done in collaboration with Montanan companies. These include 1) a demonstration of graphical inference using S2 materials, showing the potential for S2 processing to outperform conventional computing in this area; 2) a passive microwave imaging system, exploring the potential for extremely sensitive broadband S2 correlation; and 3) development of S2 processing in cryogenic waveguide devices.

Investigation of interferometric signal processing methods

Progress has been made on an interferometer setup for advanced signal processing using spectral hole burning materials. This interferometric geometry used in readout will reduce the background noise by canceling the incoherent material response while simultaneously making the coherent material response a differential signal for better selectivity of the material response. In this interferometer two beams are created using a 50/50 beamsplitter, which then transit the crystal parallel to one another and recombine coherently on the far side with a second 50/50 beamsplitter, before being detected with a balanced detector (see Figure 8.22).

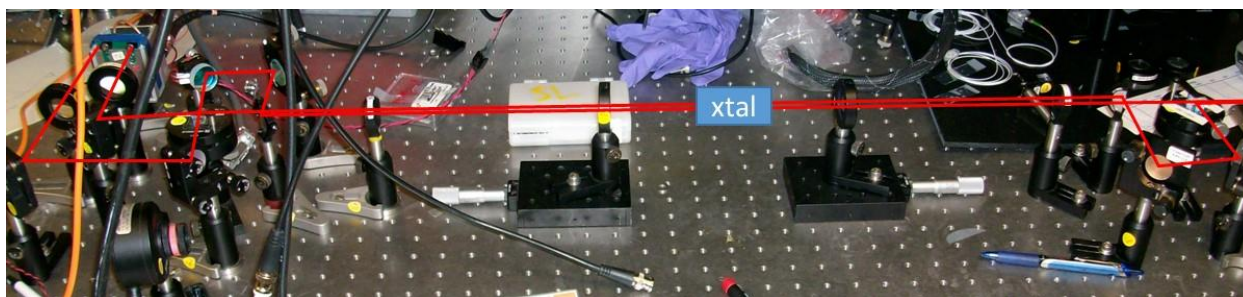


Figure 8.22. Picture of the interferometer setup with red lines representing the beams super imposed. The light paths goes from right to left.

Nondestructive characterization of optical waveguides

Previously we reported progress for using a chirped-laser, a reference fiber interferometer, and signal processing algorithms, for measuring back scattering in a waveguide to determine waveguide propagation losses without destroying the waveguide as in the typical ‘cut-back’ method for characterization. We hoped this nondestructive characterization technique would be a great way to support sales of patented chirped-laser products owned by Bridger Photonics and Blackmore. Bridger Photonics their sister company, Blackmore, are growing startup optical companies located in Bozeman. This technique would also help AdvR, another Bozeman optics company that specializes in optical waveguide manufacturing utilizing the Montana Microfabrication Facility located on the Montana State University, Bozeman campus.

An important assumption for this technique was that the waveguide propagation losses are independent of coupling losses. While this should be true for single mode waveguides, our measurements were not consistent. In particular, the waveguides in which we are able to couple well likely support a few spatial modes which can lead to different coupling efficiencies for the multiple passes in the waveguide. The smaller waveguides we are unable to couple well. We think our problem to be that the beam size focused at the input to the waveguide was too large. So, a telescope of magnification three was added to the system as shown in the Figure 8.23. This allowed us to get a tighter focus into the waveguide and better coupling.

In addition to the telescope, we added additional components to image and characterize the waveguides (see Figure 8.23). With the flip mirror up the transmitted light is incident on the power detector. As the diameter of the waveguide is changed, a change in the transmitted power is expected. With the flip mirror

down, as shown in Figure 8.23, an image of the coupled light is captured. The long pass dichroic mirror shown allows the 1545 nm light to pass and reflects wavelengths in the visible range. Coupling losses with the waveguides can be control by tuning any one of the micrometers. Unfortunately, even with these improvements our measurements again were not consistent. We believe this technique shows promise, but much more work is required to improve the measurement reliability.

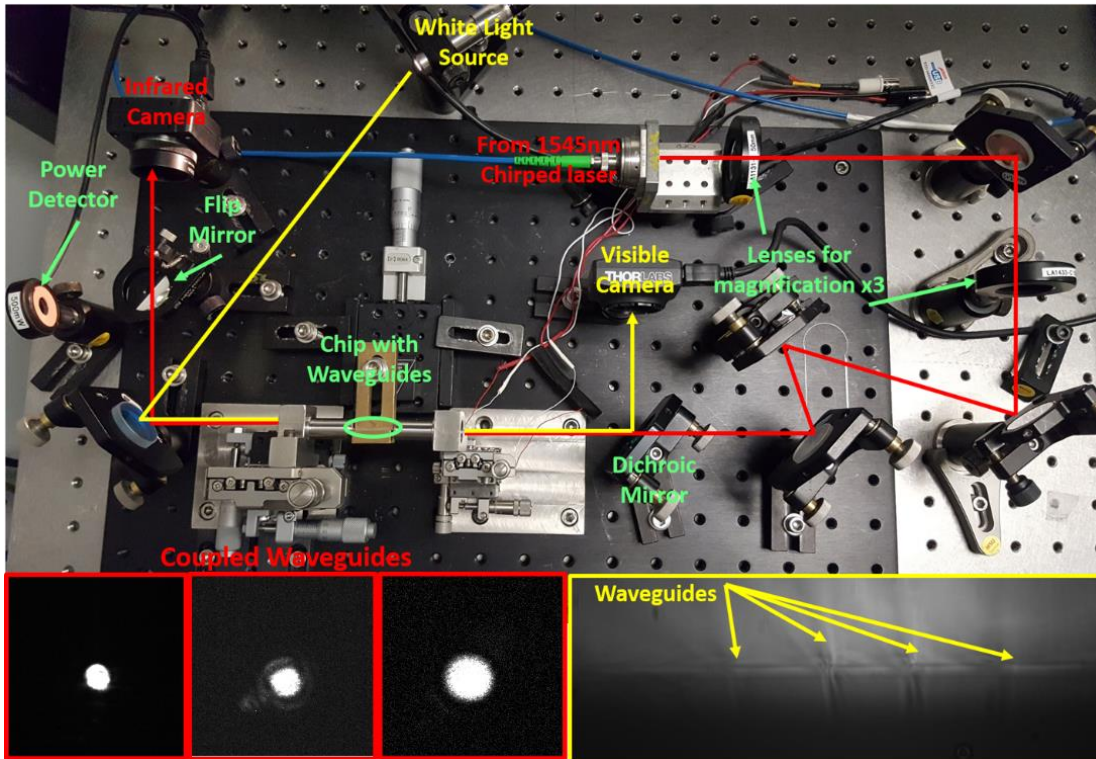


Figure 8.23. Telescope inserted into optical setup. The magnification reduced the focal point radius to $\sim 3.8 \mu\text{m}$.

Fabrication of New Waveguide Wafers

Toward the end of this quarter, Tia Sharpe of Spectrum Lab began another series of fabrication runs in the Montana Microfabrication Facility. The purpose of these runs is two-fold: to cement the techniques learned from AdvR in patterning crystalline LiNbO_3 wafers for defining waveguides, and to build a stock of patterned wafers for the Cone\Thiel group to use in developing methods to fabricate rare earth doped waveguides. The intent is to show promising results during the next quarter. The picture in Figure 17_ shows Tia Sharpe in the microfabrication facility garbed to work with acidic chemicals.

Expenditures to date (Grant 41W416) Personnel \$342,190.34, Benefits \$86,530.64, Operations \$246,715.57, Capital Equipment \$127,240.00; Total Expenditures **\$802,676.55**.



Figure 24. MSU Research Engineer Tia Sharpe in the Montana Microfabrication Facility garbed to work with chemicals for lithographic wafer processing.

Subproject 9: Optical Parametric Oscillator for Tunable Lasers (Kevin Repasky, repasky@ece.montana.edu, with AdvR, Inc.). Investigate optical parametric oscillator performance in support of characterizing large aperture periodically poled non-linear optical crystals and in support of continued development of large area methane detection.

Milestones

- a) December 2016: Model optical parametric oscillator performance using SNLO modeling tools
- b) June 30, 2017: Demonstrate singly resonant optical parametric oscillator pumped at 1064 nm and seeded at 1650 nm
- c) June 30, 2017: Final report including scientific merit and commercial products or potential

The work on the optical parametric oscillator (OPO) has met all of the milestones, as reported in the previous quarterly reports. During this quarter, the graduate student, Chat Chantjaroen, completed and successfully defended his Ph.D. thesis on April 7, 2017. During this quarter, work has begun on the next phase of the carbon dioxide (CO₂) and methane (CH₄) DIAL development. This work is focused on developing a modeling framework to aid in the final instrument design and help prepare follow-on funding requests.

Initial atmospheric modeling work was completed in order to determine the atmospheric optical depth at the proposed wavelengths. The atmospheric model was created in Matlab from code originally designed for climate modeling (<https://scienceofdoom.com/2013/01/10/visualizing-atmospheric-radiation-part-five-the-code/>). This code utilizes the HITRAN database for molecular information and incorporates standard atmospheric models. This information is used to determine temperature, pressure, and optical thickness at each layer and also a radiative transfer model to determine energy flux upwards and downwards over a range of wavelengths. The atmospheric model used for testing is based off of a standard tropical model; however, future modeling will require variable inputs in terms of pressure profiles, water vapor profiles, and molecular concentrations within each layer. The ability to modify molecular concentrations (specifically CH₄) allows different potential concentrations in the atmosphere to be modeled. For example, large concentrations of CH₄ will increase the atmospheric optical depth to the point that the range of the DIAL system is no longer limited by the output power and receiving optics, but by the atmospheric concentration. Conversely, low concentrations may not produce sufficient contrast between the On-Line and Off-Line wavelengths reducing the signal to noise of the instrument. While these are extremes that are unlikely to take place in the entire atmosphere, they may be observed in local regions of the atmosphere.

Figure 9.1 was generated using the Tropical Atmosphere model, focusing specifically on the on-line wavelength of 1645.5518 nm and the off-line wavelength of 1645.3724 nm. Figure 9.2 looks specifically at these wavelengths and shows the transparency of the off-line wavelength through the entire atmospheric column and the absorption of the on-line wavelength at lower elevations, decreasing as one moves upward through the atmosphere.

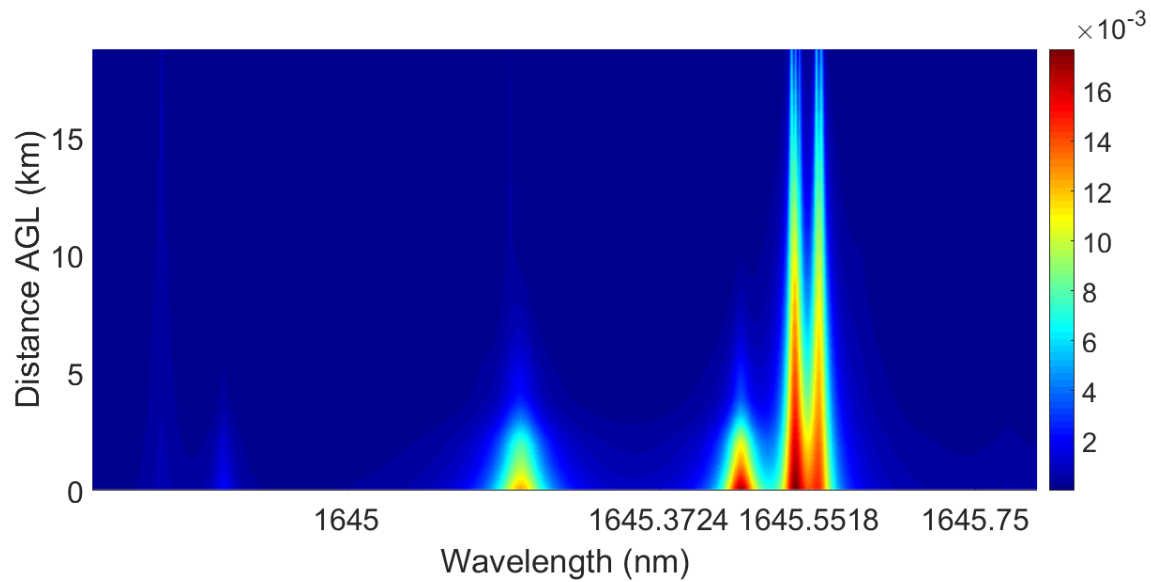


Figure 9.1: Plot of optical depth at specific wavelengths through the height of the atmosphere. Lines at 1645.3724 and 1645.5518 are the proposed Off/On lines for methane detection.

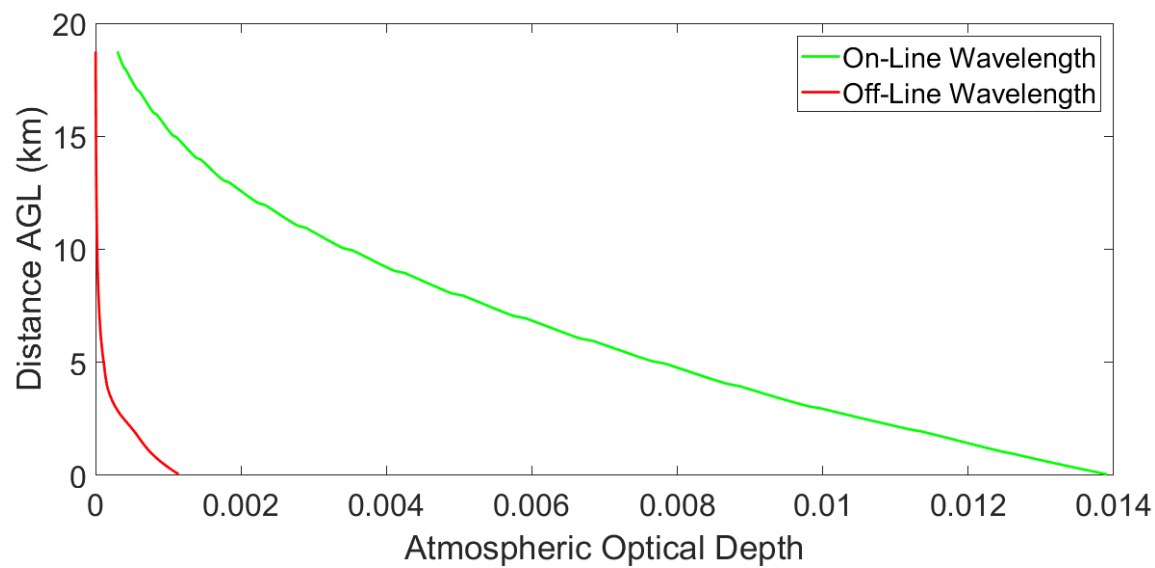


Figure 9.2: Optical depth for the On/Off Line Wavelengths as a function of height above ground level (AGL).

Lidar modeling was done using the parameters from Refaat et al., 2013 with the results shown in Figure 9.3 matching those from the paper. Future modeling will be based on the values for the proposed system and the OPO built in house. Additionally, given the speed of both the atmospheric modeling and the calculation of returns, a Monte Carlo based simulation of the various system noise parameters may be able to more directly calculate the optimal collection time, averaging time, and range binning for the system.

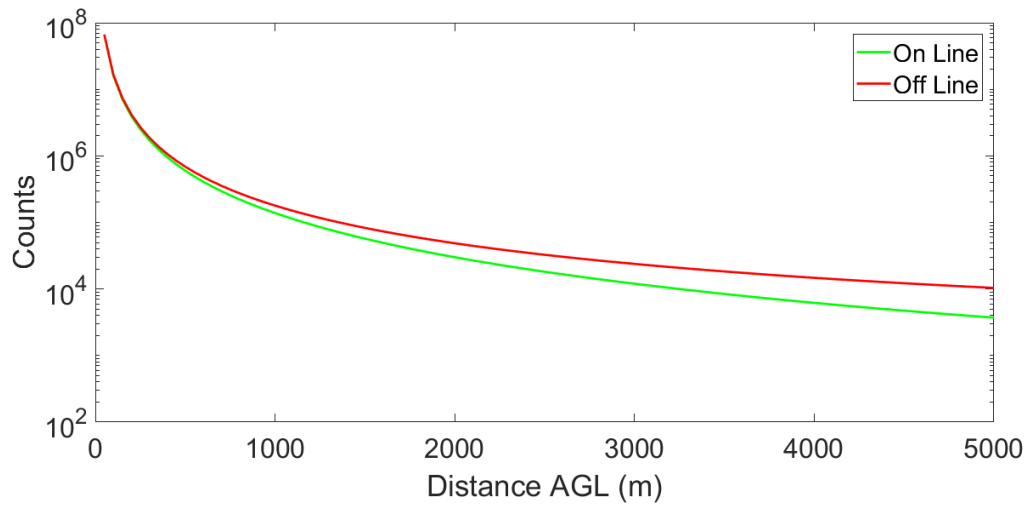


Figure 9.3: Projected return counts for the proposed Lidar system for a 1 second sampling period. Lidar parameters taken from Refaat et al., 2013.

Expenditures to date (Grant 41W412) Personnel \$56,155.55, Benefits \$3,344.75, Operations \$31,150.40; total Expenditures **\$90,650.70**.

Subproject 10: Nonlinear Optical Detection of Surface Contaminants (Rob Walker, rawalker@chemistry.montana.edu, with Altos Photonics). Develop a new method for detecting organic contaminants that accumulate on the surface of water based on nonlinear vibrational overtone spectroscopy (NVOS).

Milestones

- a) December 2015: Demonstrate feasibility of using new spectroscopic method for surface detection of adsorbed species
- b) June 2016: Submit SBIR application with Altos to develop detection and monitoring instrument based on NVOS
- c) December 2016: Successful application of NVOS to environmentally relevant systems including contaminants on water surfaces and solid substrates

Progress toward objectives

This project's goal is to develop new surface specific, optical methods capable of detecting adsorbed molecules. Specifically, our efforts are focused on exploiting the advantages of nonlinear optical spectroscopy to create a simple, sensitive technique that can identify the presence of organic contaminants at water/air and solid/liquid interfaces. Our ultimate objective is to use discoveries from our seminal studies to guide the development of portable devices capable of being used for field measurements.

The first quarter of 2017 saw significant improvement in project-specific activity as we continued to repair and recalibrate instrumentation following disruptions from dining hall construction related activities. Dust and other residue resulting from construction coupled with improved laser powers resulted in damage to optics and NLO crystals in the optical parametric amplifier. Our final service visit took place in late February. Since that time, we have re-aligned optical paths, calibrated a new detector and have begun measuring the second harmonic signals off of metal and metal oxide signals using the near-infrared light produced by ω_{signal} from the OPA. Additional work has used traditional vibrational sum frequency generation (with fixed frequency ω_{vis} and tunable ω_{IR}) to begin benchmarking vibrational signatures from lipid films adsorbed to the air/water interface. These systems were the ones that were intended for study in the original MREDI proposal. These two projects are described in more detail below.

1. Resonance enhanced SHG from metal oxide surfaces.

In the past semester, work on the SHG system in the Walker Research Group has focused on second harmonic spectra of solid-oxide fuel cell materials, including NiO, YSZ, and LSM. A crystal used to produce light in our OPerA Solo optical parametric amplifier was replaced in early February, which required a few weeks to realign after. Once we had full function of our system restored, the first experiments focused on taking baseline spectra to categorize function of the lasers and detectors after about a year of downtime due to interruptions from construction activities. Second harmonic spectra of off a non-resonant gold slide were taken at several points in the visible region of the spectrum to compare to previously acquired spectra at the same wavelengths to ensure that the system function was at or better than the level at which it had been prior to the construction.

The next experiments that were conducted were intended to look at a second harmonic signal off of a nickel oxide surface on an SOFC anode. The NiO surface was scanned with incident wavelengths between 720-620 nm, giving a SH spectrum from 360-310 nm. This region of the spectrum was chosen due to similarity with a published spectrum of a NiO surface¹ in both the fundamental and SH region. Our SH spectrum shows a strong peak at 355 nm, which corresponds well with the peak at 710 nm in the fundamental spectrum taken in the reference (Figure 10.1).

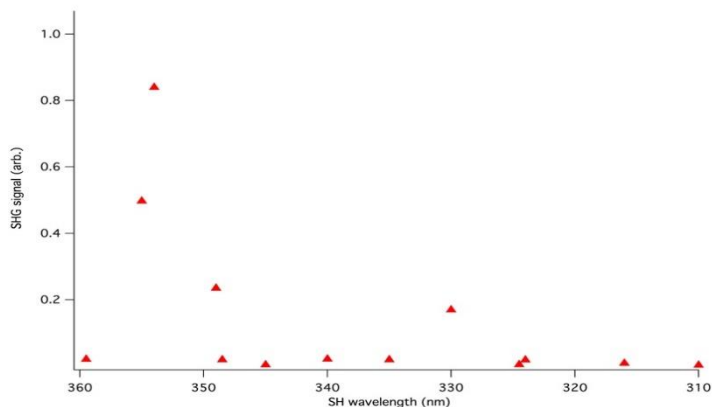


Figure 10.25: Second-harmonic spectrum of NiO surface

After successfully taking a NiO spectrum in the region of interest, the same technique was then applied to both YSZ and LSM, other common materials used in construction of SOFCs. YSZ, however, is fluorescent in the visible region, and it quickly became apparent that the background caused by that fluorescence made it so that the SH signal could not be accurately distinguished. A spectrum was taken off of LSM over a wide region of the visible spectrum (550-800 nm), but it was too porous and non-reflective to give off enough signal to make any sort of generalizations about the material (Figure 10.2). It might, however, be possible to collect SH spectra from this material in a different geometry. Future experiments will involve replicating the SH spectrum of NiO with a fundamental beam in the NIR (~1400 nm), collecting signal around 700 nm. This experiment requires realignment of the table mirrors to accommodate the new wavelength, as well as introduction of a new photomultiplier tube to collect signal at the new, higher wavelengths required. Work in the past few weeks has been focused on these modifications to allow for this next spectrum to be taken.

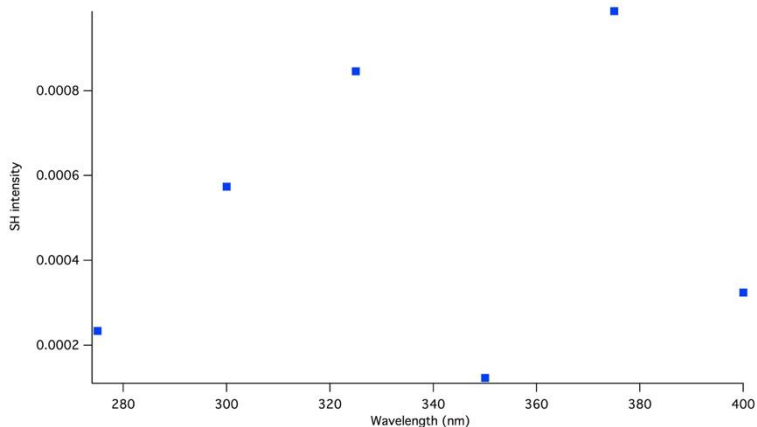


Figure 10.2: Second-harmonic spectrum of LSM surface.

2. Vibrational SFG from lipid films adsorbed to a water/air interface

VSG experiments began to investigate the hypothesis of charged based interactions with the surfactant, DPPC, by comparing the ordering of DPPC on a solution of saccharides of varying pH and charge. To investigate this hypothesis, the spectroscopic signature of the methylene and methyl groups on the lipid tail is compared. Additionally, changes in the hydroxyl stretches of water at the surface were used as another measure of ordering effects.

¹ Satoh, T., Lottermoser, T. and Fiebig, M. (2004). *Applied Physics B*. 79, 701-706.

To investigate the hypothesis that charge interaction between soluble saccharides and the lipid surfactant is the mechanism for the presence of soluble organics at ocean-like surfaces, a surface specific technique was used to analyze changes in the surface. The surfactant DPPC is zwitterionic, with a negative charge on the phosphate group and a positive charge on the amine group. Three saccharides were used: glucosamine, glucuronic acid, and N-acetyl-D-glucosamine. Glucosamine is predominately positively charged below a pH of 7.6 and predominately neutral above. Glucuronic acid is negatively charged above a pH of 3.3 and N-acetyl-D-glucosamine is predominately neutral until a pH of 11.6. Previous experiments done at both PNNL and MSU had indicated interactions between DPPC and glucosamine occurring at concentrations of glucosamine below 10 mM. For this reason, 0, 1, 2, and 10 mM concentrations of saccharides were used. For the DPPC, a surface coverage of $40 \text{ \AA}^2/\text{molecule}$ and $55 \text{ \AA}^2/\text{molecule}$ were used, corresponding to a solid and liquid condensed 2D phase.

The first set of experiments used a $40 \text{ \AA}^2/\text{molecule}$ coverage with glucosamine and glucuronic acid dissolved in Millipore water with a pH of 6 (Figure 10.3). At this pH glucosamine would be positively charged and glucuronic acid would be negatively charged. This was repeated in a 100 mM carbonate buffer at a pH of 9.5, in which glucosamine would be neutral and glucuronic acid would still be negatively charged. Spectra were taken in each condition with the physical observable being changed in the methylene and methyl symmetric stretches of the DPPC tail. Changes in these two peaks can provide a measure of order for DPPC—the methylene peak is greater in intensity when the DPPC molecules have more space and are floppy. As the DPPC becomes closer together and more ordered, the methyl peak is greater in intensity in comparison to the methylene because the DPPC are forced to maintain a tail that is more perpendicular to the water surface. This secondary effect is used to indirectly measure the interaction between the saccharides and the surfactant.

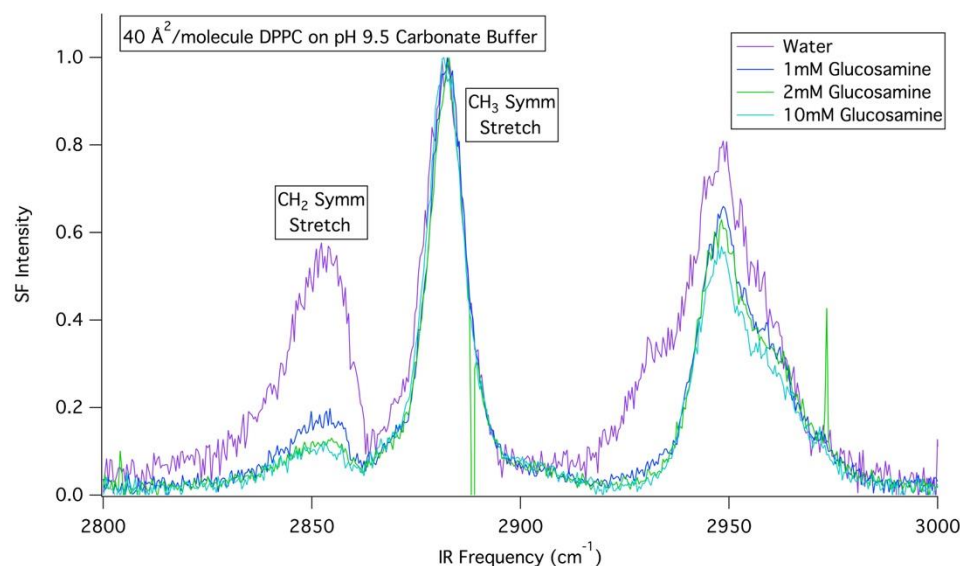


Figure 10.3: HR-BB-SFG-VS spectrum of $40 \text{ \AA}^2/\text{Molecule}$ DPPC on glucosamine solutions.

In addition to the $40 \text{ \AA}^2/\text{molecule}$ coverage of DPPC, a $55 \text{ \AA}^2/\text{molecule}$ coverage was used on solutions of 0, 1, 2 and 10 mM glucosamine and glucuronic acid at a Millipore pH of 6 (Figure 10.4). This surface coverage is of interest because the DPPC molecules have more area per DPPC molecule, so the DPPC is generally more disordered. This disorder results in spectra with intensity that is weaker than the $40 \text{ \AA}^2/\text{molecule}$ coverage, but the changes in the order due to saccharides is more pronounced.

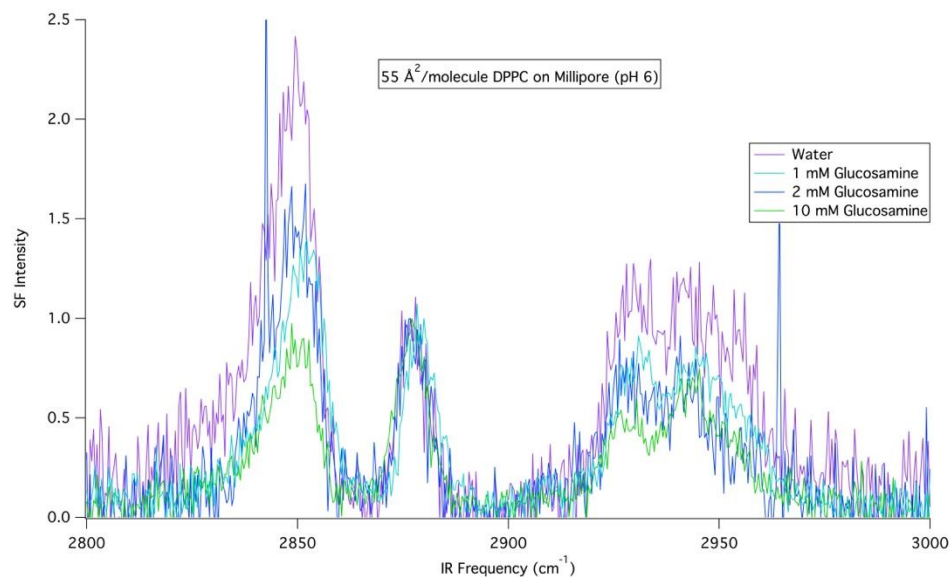


Figure 10.4: HR-BB-SFG-VS spectrum of 55 Å²/Molecule DPPC on glucosamine solutions.

The aforementioned experiments measure saccharide/lipid interactions indirectly. To get measure direct evidence of saccharides at the surface two additional experiments were done. The first experiment, using SFG, used N-acetyl-D-glucosamine as the saccharide. The acetyl group off the glucosamine had the potential to be slightly surface active so could contribute to the methyl and methylene peaks in the SFG spectra. Interestingly, at Millipore pH, no signal was found, but when the pH was increased to 11 where a greater fraction of the N-acetyl-D-glucosamine was charged there was a small SFG signal in the methylene and methyl symmetric area (Figure 10.5). Further experiments will be done to determine if the N-acetyl-D-glucosamine peaks are distinct enough from the DPPC peaks to have a direct measurement of saccharide/lipid interaction.

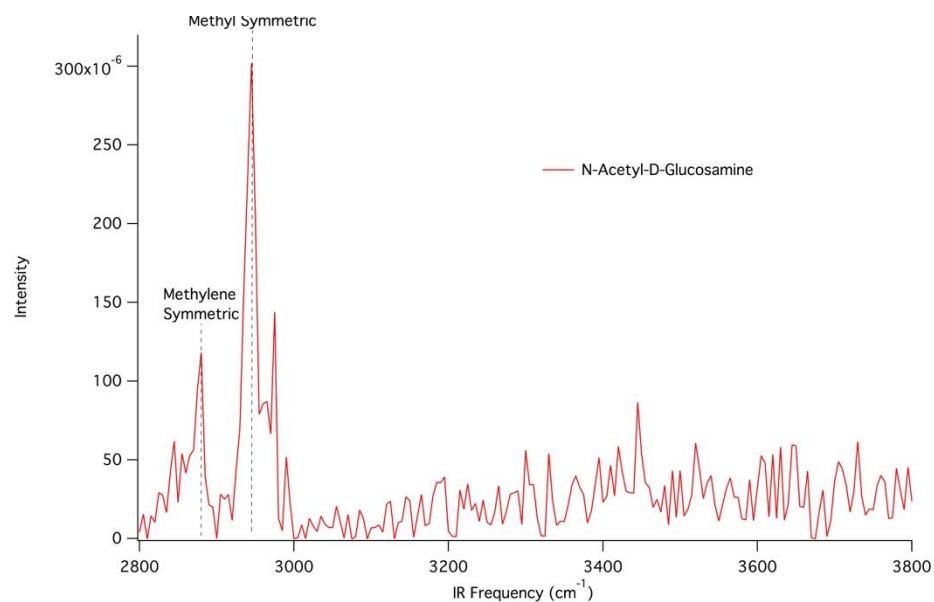


Figure 10.5: Scanning SFG spectrum of N-Acetyl-D-Glucosamine

3. Other activity (Grants preparation)

While students continued to work on making our experimental assembly functional again, I submitted one proposal to continue the work initiated with MREDI funding. The proposal was submitted to the Office of Naval Research:

ENHANCING HIGH TEMPERATURE ANODE PERFORMANCE WITH 2° ANCHORING PHASES

The proposal's project summary appears on the next page. The proposal requests \$600K (\$384K direct) over 3 years with a requested start date of July 1, 2017. The proposal is a collaborative effort between Walker (PI), Professor Stephen Sofie (Mechanical Engineering, co-PI), and Professor Roberta Amendola (Mechanical Engineering, co-PI). If awarded, this proposal will support one graduate student in the Walker Group who will continue to develop new NLO methods for studying interfaces.

A new proposal to be submitted to the ONR was begun in April, 2017 and will be submitted on May 8. This proposal will be described in the next quarterly report.

Expenditures to date (Grant 41W415) Personnel \$56,155.55, Benefits \$3,344.75, Operations \$31,150.40; total Expenditures **\$90,650.70**.